SIAM J. NUMER. ANAL.
Vol. 62, No. 1, pp. 353–375

NUMERICAL METHODS AND ANALYSIS OF COMPUTING QUASIPERIODIC SYSTEMS*

KAI JIANG†, SHIFENG LI†, AND PINGWEN ZHANG‡

Abstract. Quasiperiodic systems are important space-filling ordered structures, without decay and translational invariance. How to solve quasiperiodic systems accurately and efficiently is a great challenge. A useful approach, the projection method (PM) [*J. Comput. Phys.*, 256 (2014), pp. 428–440], has been proposed to compute quasiperiodic systems. Various studies have demonstrated that the PM is an accurate and efficient method to solve quasiperiodic systems. However, there is a lack of theoretical analysis of the PM. In this paper, we present a rigorous convergence analysis of the PM by establishing a mathematical framework of quasiperiodic functions and their high-dimensional periodic functions. We also give a theoretical analysis of the quasiperiodic spectral method (QSM) based on this framework. Results demonstrate that the PM and QSM both have exponential decay, and the QSM (PM) is a generalization of the periodic Fourier spectral (pseudospectral) method. Then, we analyze the computational complexity of the PM and QSM in calculating quasiperiodic systems. The PM can use a fast Fourier transform, while the QSM cannot. Moreover, we investigate the accuracy and efficiency of the PM, QSM, and periodic approximation method in solving the linear time-dependent quasiperiodic Schrödinger equation.

Key words. quasiperiodic systems, quasiperiodic spectral method, projection method, Birkhoff's ergodic theorem, error estimation, time-dependent quasiperiodic Schrodinger equation

MSC codes. 42A75, 65T40, 68W40, 74S25

DOI. 10.1137/22M1524783

1. Introduction.

Quasiperiodic systems are a natural extension of periodic systems. The earliest quasiperiodic system can be traced back to the study of the three-body problem [1]. Many physical systems can fall into the set of quasiperiodicity, including periodic systems, incommensurate structures, quasicrystals, many-body problems, polycrystalline materials, and quasiperiodic quantum systems [1, 2, 3, 4]. The mathematical study of quasiperiodic orders is a beautiful synthesis of geometry, analysis, algebra, dynamic system, and number theory [5, 6]. The theory of quasiperiodic functions, even more general almost periodic functions, has been well developed to study quasiperiodic systems in mathematics [7, 8, 9]. However, how to numerically solve quasiperiodic systems in an accurate and efficient way is still a great challenge.

Generally speaking, quasiperiodic systems, related to irrational numbers, are space-filling ordered structures without decay or translational invariance. This raises difficulty in numerically computing quasiperiodic systems. To study such important systems, several numerical methods have been developed. A widely used approach, the

*Received by the editors September 26, 2022; accepted for publication (in revised form) November 7, 2023; published electronically February 1, 2024.
https://doi.org/10.1137/22M1524783
Funding: The work of the authors was supported by the National K&D Program of China (2023YFA1008802), the National Natural Science Foundation of China grants 12171412 and 12288101. The work of the first author was also partially supported by the Natural Science Foundation for Distinguished Young Scholars of Hunan Province of China grant 2021JJ10037.
†Hunan Key Laboratory for Computation and Simulation in Science and Engineering, Key Laboratory of Intelligent Computing and Information Processing of Ministry of Education, School of Mathematics and Computational Science, Xiangtan University, Xiangtan, Hunan 411105 China (kaijiang@xtu.edu.cn, shifengli@smail.xtu.edu.cn).
‡School of Mathematics and Statistics, Wuhan University, Wuhan 430072 China and School of Mathematical Sciences, Peking University, Beijing 100871 China (pzhang@pku.edu.cn).

periodic approximation method (PAM), employs a periodic function to approximate the quasiperiodic function [10]. The conventional viewpoint is that the approximation error could uniformly decay as the supercell gradually becomes large. However, a recent theoretical analysis has demonstrated that the error of the PAM may not uniformly decrease as the calculation area increases [11]. The second method is the quasiperiodic spectral method (QSM), which approximates a quasiperiodic function by a finite summation of trigonometric polynomials based on the continuous Fourier–Bohr transform [10]; see also subsection 3.1. The third approach is the projection method (PM) [12], based on the fact that the quasiperiodic system can be embedded into a high-dimensional periodic system. Then, the PM can accurately calculate the high-dimensional periodic system over a torus in a pseudospectral manner. Meanwhile, the PM is efficient due to the availability of a fast Fourier transform (FFT). Finally, the PM obtains the quasiperiodic system by choosing a corresponding irrational slice of the high-dimensional torus by the projection matrix. Extensive studies have demonstrated that the PM can be used to compute quasiperiodic systems to high precision, including quasicrystals [13, 14], incommensurate quantum systems [15, 16, 17], topological insulators [18], and grain boundaries [19, 20]. However, the PM still has a lack of corresponding theoretical guarantees.

In this work, we present a rigorous theoretical analysis of numerical methods for solving quasiperiodic systems. We establish the relationship between quasiperiodic functions and their corresponding high-dimensional periodic functions based on the idea of the PM. These mathematical results provide a theoretical framework to analyze the convergence of the PM, as well as the QSM. We also present another error analysis framework of the QSM without using high-dimensional periodic functions. These theoretical results demonstrate that both the PM and QSM have exponential convergence. Moreover, we analyze the computational complexity of the PM and QSM in solving quasiperiodic systems. The PM can use an FFT by introducing discrete Fourier–Bohr transform (see subsection 3.2), while the QSM cannot. Further analysis reveals that the QSM (PM) is an extension of the periodic Fourier spectral (pseudospectral) method. Finally, we investigate the accuracy and efficiency of the PM, QSM, and PAM in solving the linear time-dependent quasiperiodic Schrödinger equation (TQSE).

2. Preliminaries.

Before our analysis, we give some preliminaries on quasiperiodic and periodic functions in this section.

2.1. Preliminaries of quasiperiodic functions.

Let us recall the definition of the quasiperiodic function [9]. Denote

$$\mathbb{M}^{d\times n} = \{\boldsymbol{M} = (\boldsymbol{m}_1, \dots, \boldsymbol{m}_n) \in \mathbb{R}^{d\times n} : \boldsymbol{m}_1, \dots, \boldsymbol{m}_n \text{ are } \mathbb{Q}\text{-linearly independent}\},$$

and define $\boldsymbol{P} \in \mathbb{M}^{d\times n}$ as the projection matrix.

DEFINITION 2.1. *A d-dimensional function $f(\boldsymbol{x})$ is quasiperiodic if there exists a continuous n-dimensional periodic function F $(n \geq d)$ that satisfies $f(\boldsymbol{x}) = F(\boldsymbol{P}^T\boldsymbol{x})$, where $\boldsymbol{P}$ is the projection matrix.*

In particular, when $n = d$ and $\boldsymbol{P}$ is nonsingular, $f(\boldsymbol{x})$ is periodic. When $n \to \infty$, f is an almost periodic function [7]. For convenience, F in Definition 2.1 is called the parent function of f in the following content. $\mathrm{QP}(\mathbb{R}^d)$ represents the space of all quasiperiodic functions. In section 4, we will show that f and F can be uniquely determined by each other when the projection matrix $\boldsymbol{P}$ is given.

Let $K_T=\{\boldsymbol{x}:\boldsymbol{x}\in\mathbb{R}^d,\ |x_j|\le T,\ j=1,\dots,d\}$ be the cube in $\mathbb{R}^d$. The mean value $\mathcal{M}\{f(\boldsymbol{x})\}$ of $f\in\mathrm{QP}(\mathbb{R}^d)$ is defined as

$$\mathcal{M}\{f(\boldsymbol{x})\}=\lim_{T\to+\infty}\frac{1}{(2T)^d}\int_{\boldsymbol{s}+K_T}f(\boldsymbol{x})\,d\boldsymbol{x}:=\fint f(\boldsymbol{x})\,d\boldsymbol{x},$$

where the limit on the right side exists uniformly for all $\boldsymbol{s}\in\mathbb{R}^d$. An elementary calculation shows that

$$\mathcal{M}\{e^{i\boldsymbol{\lambda}^T\boldsymbol{x}}e^{-i\boldsymbol{\beta}^T\boldsymbol{x}}\}=\begin{cases}1, & \boldsymbol{\lambda}=\boldsymbol{\beta},\\ 0, & \boldsymbol{\lambda}\neq\boldsymbol{\beta}.\end{cases}\tag{2.1}$$

Correspondingly, the continuous Fourier–Bohr transform of $f(\boldsymbol{x})$ is

$$\hat{f}_{\boldsymbol{\lambda}}=\mathcal{M}\{f(\boldsymbol{x})e^{-i\boldsymbol{\lambda}^T\boldsymbol{x}}\},\tag{2.2}$$

where $\boldsymbol{\lambda}\in\mathbb{R}^d$. Denote $\boldsymbol{\Lambda}=\{\boldsymbol{\lambda}:\boldsymbol{\lambda}=\boldsymbol{P}\boldsymbol{k},\ \boldsymbol{k}\in\mathbb{Z}^n\}$, and the Fourier series associated with the quasiperiodic function $f(\boldsymbol{x})$ can be written as

$$f(\boldsymbol{x})\sim\sum_{\boldsymbol{k}\in\mathbb{Z}^n}\hat{f}_{\boldsymbol{\lambda}_{\boldsymbol{k}}}e^{i\boldsymbol{\lambda}_{\boldsymbol{k}}^T\boldsymbol{x}},\tag{2.3}$$

where $\boldsymbol{\lambda}_{\boldsymbol{k}}=\boldsymbol{P}\boldsymbol{k}\in\boldsymbol{\Lambda}$ are Fourier exponents and $\hat{f}_{\boldsymbol{\lambda}_{\boldsymbol{k}}}$ (defined in (2.2)) are Fourier coefficients. To simplify the notation, denote $\hat{f}_{\boldsymbol{k}}=\hat{f}_{\boldsymbol{\lambda}_{\boldsymbol{k}}}$. Let

$$\mathrm{QP}_1(\mathbb{R}^d)=\left\{f\in\mathrm{QP}(\mathbb{R}^d):\sum_{\boldsymbol{k}\in\mathbb{Z}^n}|\hat{f}_{\boldsymbol{k}}|<+\infty\right\},$$

with norm $\|f\|_{\mathcal{L}^\infty(\mathbb{R}^d)}=\sup_{\boldsymbol{x}\in\mathbb{R}^d}|f(\boldsymbol{x})|$.

In general, the convergence of the Fourier series (2.3) is a challenging problem; see [9] for some sufficient criteria. The following conclusion presents an important convergence property of a quasiperiodic function.

Theorem 2.2 ([25], Chapter 1.3). *If the Fourier series of a quasiperiodic function is uniformly convergent, then the sum of the series is the given function.*

If the Fourier series of the quasiperiodic function is absolutely convergent, it is also uniformly convergent. Therefore, for $f\in\mathrm{QP}_1(\mathbb{R}^d)$, we have

$$f(\boldsymbol{x})=\sum_{\boldsymbol{k}\in\mathbb{Z}^n}\hat{f}_{\boldsymbol{k}}e^{i\boldsymbol{\lambda}_{\boldsymbol{k}}^T\boldsymbol{x}}.$$

As a consequence, we can obtain a subspace $\mathrm{QP}_2(\mathbb{R}^d)$ of $\mathrm{QP}(\mathbb{R}^d)$

$$\mathrm{QP}_2(\mathbb{R}^d)=\left\{f\in\mathrm{QP}(\mathbb{R}^d):\mathcal{M}\{|f|^2\}<+\infty\right\}$$

equipped with norm

$$\|f\|^2_{\mathcal{L}^2(\mathbb{R}^d)}=\mathcal{M}\{|f|^2\}=\sum_{\boldsymbol{k}\in\mathbb{Z}^n}|\hat{f}_{\boldsymbol{k}}|^2\tag{2.4}$$

and the inner product $(\cdot,\cdot)_{QP_2(\mathbb{R}^d)}$

$$(f_1,f_2)_{QP_2(\mathbb{R}^d)}=\fint f_1(\boldsymbol{x})\bar{f}_2(\boldsymbol{x})\,d\boldsymbol{x}.$$

Equality (2.4) is Parseval's identity. Now we introduce the Hilbert space of quasiperiodic functions. Denote $|\boldsymbol{x}| = \sum_{j=1}^{d} |x_j|$ with for all $\boldsymbol{x} \in \mathbb{R}^d$. For any $m \in \mathbb{N}_0 = \{m \in \mathbb{Z} : m > 0\}$, the Sobolev space $H^{\alpha}_{QP}(\mathbb{R}^d)$ comprises all quasiperiodic functions with partial derivatives order $\alpha \geq 1$ with respect to the inner product $(\cdot,\cdot)_\alpha$

$$(f_1, f_2)_\alpha = (f_1, f_2)_{QP_2(\mathbb{R}^d)} + \sum_{|m|=\alpha} (\partial^m_{\boldsymbol{x}} f_1, \partial^m_{\boldsymbol{x}} f_2)_{QP_2(\mathbb{R}^d)}$$

and endowed with norm $\|f\|^2_\alpha = \sum_{\boldsymbol{k}\in\mathbb{Z}^n} (1 + |\boldsymbol{\lambda_k}|^2)^\alpha |\hat{f}_{\boldsymbol{k}}|^2$ and seminorm $|f|^2_\alpha = \sum_{\boldsymbol{k}\in\mathbb{Z}^n} |\boldsymbol{\lambda_k}|^{2\alpha} |\hat{f}_{\boldsymbol{k}}|^2$.

2.2. Preliminaries of periodic functions. Let $\mathbb{T}^n = (\mathbb{R}/2\pi\mathbb{Z})^n$ be the n-dimensional torus; then the Fourier transform of $F(\boldsymbol{y})$ defined on $\mathbb{T}^n$

$$\hat{F}_{\boldsymbol{k}} = \frac{1}{|\mathbb{T}^n|} \int_{\mathbb{T}^n} e^{-i\boldsymbol{k}^T\boldsymbol{y}} F(\boldsymbol{y})\, d\boldsymbol{y}, \ \ \boldsymbol{k} \in \mathbb{Z}^n, \tag{2.5}$$

and

$$L^\infty(\mathbb{T}^n) = \left\{ F(\boldsymbol{y}) : \sum_{\boldsymbol{k}\in\mathbb{Z}^n} |\hat{F}_{\boldsymbol{k}}| < +\infty \right\}.$$

Furthermore, denote the Hilbert space on $\mathbb{T}^n$

$$L^2(\mathbb{T}^n) = \Big\{ F(\boldsymbol{y}) : \langle F, F\rangle < +\infty \Big\},$$

equipped with inner product

$$\langle F_1, F_2 \rangle = \frac{1}{|\mathbb{T}^n|} \int_{\mathbb{T}^n} F_1 \bar{F}_2 \, d\boldsymbol{y}.$$

For any integer $\alpha \geq 0$, the α-derivative Sobolev space on $\mathbb{T}^n$ is

$$H^\alpha(\mathbb{T}^n) = \{F \in L^2(\mathbb{T}^n) : \|F\|_\alpha < \infty\},$$

where $\|F\|_\alpha = \left(\sum_{\boldsymbol{k}\in\mathbb{Z}^n} (1 + \|\boldsymbol{k}\|_2^{2\alpha}) |\hat{F}_{\boldsymbol{k}}|^2\right)^{1/2}$, with $\|\boldsymbol{k}\|_2^2 = \sum_{j=1}^n |k_j|^2$. The seminorm of $H^\alpha(\mathbb{T}^n)$ can be defined as $|F|_\alpha = \left(\sum_{\boldsymbol{k}\in\mathbb{Z}^n} \|\boldsymbol{k}\|_2^{2\alpha} |\hat{F}_{\boldsymbol{k}}|^2\right)^{1/2}$.

3. Algorithms.

In this paper, our purpose is to establish the theoretical analysis of the QSM and PM. In this section, we introduce these algorithms before delving into the numerical analysis. Moreover, we present the implementation framework of the PM by defining the discrete Fourier–Bohr transform of quasiperiodic functions.

For an integer $N \in \mathbb{N}_0$ and a given projection matrix $\boldsymbol{P} \in \mathbb{M}^{d\times n}$, denote

$$K^n_N = \{\boldsymbol{k} = (k_j)_{j=1}^n \in \mathbb{Z}^n : -N \leq k_j < N\}$$

and

$$\boldsymbol{\Lambda}^d_N = \{\boldsymbol{\lambda} = \boldsymbol{P}\boldsymbol{k} : \boldsymbol{k} \in K^n_N\} \subset \boldsymbol{\Lambda}. \tag{3.1}$$

Obviously, the order of the set $\boldsymbol{\Lambda}^d_N$ is $\#(\boldsymbol{\Lambda}^d_N) = (2N)^n$. The finite dimensional linear subspace of $\mathrm{QP}(\mathbb{R}^d)$ is

$$S_N = \mathrm{span}\{e^{i\boldsymbol{\lambda}^T\boldsymbol{x}},\ \boldsymbol{x} \in \mathbb{R}^d,\ \boldsymbol{\lambda} \in \boldsymbol{\Lambda}^d_N\}.$$

We denote $\mathcal{P}_N : \mathrm{QP}(\mathbb{R}^d) \mapsto S_N$ the projection operator. For a quasiperiodic function $f(\boldsymbol{x}) \in \mathrm{QP}_1(\mathbb{R}^d)$ and its Fourier exponent $\boldsymbol{\lambda_k} \in \boldsymbol{\Lambda}$, we can split it into two parts:

$$f(\boldsymbol{x}) = \sum_{\boldsymbol{k}\in K_N^n} \hat{f}_{\boldsymbol{k}} e^{i\boldsymbol{\lambda}_{\boldsymbol{k}}^T \boldsymbol{x}} + \sum_{\boldsymbol{k}\in \mathbb{Z}^n/K_N^n} \hat{f}_{\boldsymbol{k}} e^{i\boldsymbol{\lambda}_{\boldsymbol{k}}^T \boldsymbol{x}} = \mathcal{P}_N f + (f - \mathcal{P}_N f). \tag{3.2}$$

Next, we present the QSM and PM, respectively.

3.1. Quasiperiodic spectral method. The QSM directly approximates the quasiperiodic function f by $\mathcal{P}_N f$,

$$f(\boldsymbol{x}) \approx \mathcal{P}_N f(\boldsymbol{x}) = \sum_{\boldsymbol{k}\in K_N^n} \hat{f}_{\boldsymbol{k}} e^{i\boldsymbol{\lambda}_{\boldsymbol{k}}^T \boldsymbol{x}}, \quad \boldsymbol{x} \in \mathbb{R}^d,$$

where the quasiperiodic Fourier coefficient $\hat{f}_{\boldsymbol{k}}$ is obtained by the continuous Fourier–Bohr transform (2.2). We will give the error analysis of the QSM in subsection 5.1 and describe the numerical implementation of solving a quasiperiodic system in subsection 6.1.1. Note that quasiperiodic Fourier coefficients in the QSM are obtained through the continuous Fourier–Bohr transform (2.2), resulting in the QSM being unable to use an FFT. A further computational complexity analysis will be presented in subsection 6.1.1.

3.2. Projection method. The PM embeds the quasiperiodic function $f(\boldsymbol{x})$ into a high-dimensional parent function $F(\boldsymbol{y})$, then directly replaces the discrete quasiperiodic Fourier coefficients with the discrete parent Fourier coefficients [10, 12]. We can use the periodic Fourier spectral method to obtain the parent Fourier coefficients. Concretely, we first discretize the tours $\mathbb{T}^n$. Without loss of generality, we consider a fundamental domain $[0, 2\pi)^n$ and assume that the discrete nodes in each dimension are the same, i.e., $N_1 = N_2 = \cdots = N_n = 2N$, $N \in \mathbb{N}_0$. The spatial discrete size $h = \pi/N$. The spatial variables are evaluated on the standard numerical grid $\mathbb{T}_N^n$ with grid points $\boldsymbol{y_j} = (y_{1,j_1}, y_{2,j_2}, \ldots, y_{n,j_n})$, $y_{1,j_1} = j_1 h$, $y_{2,j_2} = j_2 h, \ldots, y_{n,j_n} = j_n h$, $0 \le j_1, j_2, \ldots, j_n < 2N$. We define the grid function space

$$\mathcal{G}_N := \{F : \mathbb{Z}^n \mapsto \mathbb{C} : \ F \text{ is } \mathbb{T}_N^n\text{-periodic}\}.$$

Given any periodic grid functions $F, G \in \mathcal{G}_N$, the ℓ^2-inner product is defined as

$$\langle F, G\rangle_N = \frac{1}{(4\pi N)^n} \sum_{\boldsymbol{y_j}\in\mathbb{T}_N^n} F(\boldsymbol{y_j})\overline{G}(\boldsymbol{y_j}).$$

For $\boldsymbol{k}, \boldsymbol{\ell} \in \mathbb{Z}^n$, we have the discrete orthogonality condition

$$\langle e^{i\boldsymbol{k}^T\boldsymbol{y_j}}, e^{i\boldsymbol{\ell}^T\boldsymbol{y_j}}\rangle_N = \begin{cases} 1, & \boldsymbol{k} = \boldsymbol{\ell} + 2N\boldsymbol{m},\ \boldsymbol{m} \in \mathbb{Z}^n, \\ 0, & \text{otherwise.} \end{cases} \tag{3.3}$$

The discrete Fourier coefficient of $F \in \mathcal{G}_N$ is

$$\tilde{F}_{\boldsymbol{k}} = \langle F, e^{i\boldsymbol{k}^T\boldsymbol{y_j}}\rangle_N, \quad \boldsymbol{k} \in K_N^n. \tag{3.4}$$

The PM directly takes $\tilde{f}_{\boldsymbol{k}} = \tilde{F}_{\boldsymbol{k}}$. We define the *discrete Fourier–Bohr transform* of quasiperiodic function $f(\boldsymbol{x})$ as

$$f(\boldsymbol{x_j}) = \sum_{\boldsymbol{\lambda_k}\in\boldsymbol{\Lambda}_N^d} \tilde{f}_{\boldsymbol{k}} e^{i\boldsymbol{\lambda}_{\boldsymbol{k}}^T \boldsymbol{x_j}}, \tag{3.5}$$

where *collocation points* $\boldsymbol{x_j} = \boldsymbol{P}\boldsymbol{y_j}$, $\boldsymbol{y_j} \in \mathbb{T}_N^n$. The trigonometric interpolation of quasiperiodic function is

$$I_N f(\boldsymbol{x}) = \sum_{\boldsymbol{\lambda_k} \in \boldsymbol{\Lambda}_N^d} \tilde{f}_{\boldsymbol{k}} e^{i\boldsymbol{\lambda}_{\boldsymbol{k}}^T \boldsymbol{x}}. \tag{3.6}$$

Consequently, $I_N f(\boldsymbol{x}_j) = f(\boldsymbol{x}_j)$. From the implementation, the PM can use the n-dimensional FFT to obtain quasiperiodic Fourier coefficients by introducing the discrete Fourier–Bohr transform (3.5). The concrete computational complexity of the PM for solving quasiperiodic systems will be shown in subsection 6.1.2.

Remark 3.1. From the above description, the QSM and PM are generalizations of the Fourier spectral method and Fourier pseudospectral method, respectively. When $f(\boldsymbol{x})$ is periodic, i.e., $n = d$ and the projection matrix $\boldsymbol{P} \in \mathbb{M}^{d\times d}$ is nonsingular, the QSM (PM) reduces to the periodic Fourier spectral (pseudospectral) method.

4. Theoretical framework.

From the implementation framework of the PM presented in subsection 3.2, exploring the relationship between quasiperiodic functions and their parent functions is a prerequisite for its convergence analysis. Here, we prove that the quasiperiodic Fourier coefficients $\hat{f}_{\boldsymbol{k}}$ of (2.2) are equal to their parent Fourier coefficients $\hat{F}_{\boldsymbol{k}}$ of (2.5).

THEOREM 4.1. *For a given quasiperiodic function*

$$f(\boldsymbol{x}) = F(\boldsymbol{P}^T\boldsymbol{x}), \quad \boldsymbol{x} \in \mathbb{R}^d,$$

where $F(\boldsymbol{y})$ is its parent function defined on the tours $\mathbb{T}^n$ and $\boldsymbol{P}$ is the projection matrix, we have

$$\hat{f}_{\boldsymbol{k}} = \hat{F}_{\boldsymbol{k}}, \quad \boldsymbol{k} \in \mathbb{Z}^n, \tag{4.1}$$

where $\hat{f}_{\boldsymbol{k}}$ and $\hat{F}_{\boldsymbol{k}}$ are defined by (2.2) *and* (2.5), *respectively.*

We will prove Theorem 4.1 based on Birkhoff's ergodic theorem [26, 27]. Let us start with some basic definitions. Let Ω be a set. A σ-algebra of Ω is a collection $\mathcal{B}$ of subsets of Ω satisfying the following three conditions: (i) $\Omega \in \mathcal{B}$; (ii) if $B \in \mathcal{B}$, then $\Omega \backslash B \in \mathcal{B}$; (iii) if $B_n \in \mathcal{B}$ for $n \geq 1$, then $\bigcup_{n=1}^{\infty} B_n \in \mathcal{B}$. We call the pair $(\Omega, \mathcal{B})$ a measurable space. The Lebesgue measure on $(\Omega, \mathcal{B})$ is a function $\mu : \mathcal{B} \mapsto \mathbb{R}^+$ satisfying $\mu(\emptyset) = 0$ and $\mu(\bigcup_{n=1}^{\infty} B_n) = \sum_{n=1}^{\infty} \mu(B_n)$ whenever $\{B_n\}_{n=1}^{\infty}$ is a sequence of members of $\mathcal{B}$ that are pairwise disjoint subsets of Ω. A finite measure space is a triple $(\Omega, \mathcal{B}, \mu)$, where $(\Omega, \mathcal{B})$ is a measurable space and μ is a finite measure on $(\Omega, \mathcal{B})$. We say that $(\Omega, \mathcal{B}, \mu)$ is a probability space or a normalized measure space if $\mu(\Omega) = 1$.

DEFINITION 4.2. *Suppose that $(\Omega_1, \mathcal{B}_1, \mu_1)$ and $(\Omega_2, \mathcal{B}_2, \mu_2)$ are probability spaces.*

(i) *A transformation $\phi : \Omega_1 \mapsto \Omega_2$ is a measure if $\phi^{-1}(\mathcal{B}_2) \subset \mathcal{B}_1$;*
(ii) *A transformation $\phi : \Omega_1 \mapsto \Omega_2$ is measure-preserving if ϕ is measureable and $\mu_1(\phi^{-1}B_2) = \mu_2(B_2)$, for each $B_2 \in \mathcal{B}_2$.*

DEFINITION 4.3. *Let $(\Omega, \mathcal{B}, \mu)$ be a probability space. A measure-preserving transformation $\phi : \Omega \mapsto \Omega$ is called ergodic if the only member $B \in \mathcal{B}$ with $\phi^{-1}B = B$ satisfying $\mu(B) = 1$ or $\mu(B) = 0$.*

Lemma 4.1 gives an equivalent condition of ergodicity.

LEMMA 4.1 (Theorem 1.6 [26]). *Let $(\Omega, \mathcal{B}, \mu)$ be a probability space, and let $\phi : \Omega \mapsto \Omega$ be measure-preserving mapping; then the following statements are equivalent:*

(i) *ϕ is ergodic;*

(ii) *If f is measurable and $f \circ \phi = f$ a.e., then f is constant a.e.*

The high-dimensional Birkhoff's ergodic theorem reads as follows.

THEOREM 4.4 ([27]). *Let $f(\boldsymbol{z}) : \Omega \mapsto \mathbb{C}$ be integrable, and let the measure-preserving transformation $\phi^{\boldsymbol{x}}$, $\boldsymbol{x} \in \mathbb{R}^d$ satisfy*

$$\phi^{\boldsymbol{0}}\boldsymbol{z} = \boldsymbol{z}, \;\; \phi^{\boldsymbol{x}_1+\boldsymbol{x}_2}\boldsymbol{z} = \phi^{\boldsymbol{x}_1}(\phi^{\boldsymbol{x}_2}\boldsymbol{z}), \;\; \boldsymbol{z} \in \Omega$$

for any $\boldsymbol{x}_1, \boldsymbol{x}_2 \in \mathbb{R}^d$. Then,

$$⨍ f(\phi^{\boldsymbol{x}}\boldsymbol{z})\, d\boldsymbol{x} = f^*(\boldsymbol{z})$$

exists for almost all $\boldsymbol{z}$ in Ω. Moreover,

$$\int_E f^*(\boldsymbol{z})\, d\boldsymbol{z} = \int_E f(\boldsymbol{z})\, d\boldsymbol{z},$$

where $E \subset \Omega$ is the invariant subset under $\phi^{\boldsymbol{x}}$.

In this work, $\Omega = E = \mathbb{T}^n$. Given a projection matrix $\boldsymbol{P} = (\boldsymbol{p}_1, \boldsymbol{p}_2, \ldots, \boldsymbol{p}_n) \in \mathbb{M}^{d\times n}$, denote the parameterized translation

$$\phi^{\boldsymbol{x}}_{\boldsymbol{P}}(z_1, \ldots, z_n) = (z_1 + \boldsymbol{p}_1^T\boldsymbol{x}, \ldots, z_n + \boldsymbol{p}_n^T\boldsymbol{x})\; (mod\, 1), \tag{4.2}$$

where "*mod* 1" means that each coordinate remains its fractional part. Proposition 4.2 will show that $\phi^{\boldsymbol{x}}_{\boldsymbol{P}}$ is ergodic in probability space $(\mathbb{T}^n, \mathcal{B}, \mu)$ when μ is a Lebesgue measure.

PROPOSITION 4.2. *If $\boldsymbol{P} \in \mathbb{M}^{d\times n}$, then the parameterized translation $\phi^{\boldsymbol{x}}_{\boldsymbol{P}}$ defined by* (4.2) *is ergodic with respect to the Lebesgue measure.*

Proof. The parameterized translation $\phi^{\boldsymbol{x}}_{\boldsymbol{P}}$ is measure-preserving with respect to the Lebesgue measure μ. The torus $\mathbb{T}^n$ is an invariant set under the translation $\phi^{\boldsymbol{x}}_{\boldsymbol{P}}$ since $\phi^{\boldsymbol{x}}_{\boldsymbol{P}}(\boldsymbol{z}) \in \mathbb{T}^n$ for each $\boldsymbol{z} \in \mathbb{T}^n$. Let χ be a bounded measurable function invariant under $\phi^{\boldsymbol{x}}_{\boldsymbol{P}}$, for example, the characteristic function of an invariant set $\mathbb{T}^n$. Then, we have

$$\chi_{\mathbb{T}^n}(\phi^{\boldsymbol{x}}_{\boldsymbol{P}}(\boldsymbol{z})) = \chi_{(\phi^{\boldsymbol{x}}_{\boldsymbol{P}})^{-1}(\mathbb{T}^n)}(\boldsymbol{z}) = \chi_{\mathbb{T}^n}(\boldsymbol{z}). \tag{4.3}$$

Without causing confusion, (4.3) can be rewritten as $\chi(\phi^{\boldsymbol{x}}_{\boldsymbol{P}}(\boldsymbol{z})) = \chi(\boldsymbol{z})$. Considering the Fourier expansion of χ,

$$\chi(\boldsymbol{z}) = \sum_{\boldsymbol{k}\in\mathbb{Z}^n} \hat{\chi}_{\boldsymbol{k}} e^{i\boldsymbol{k}^T\boldsymbol{z}},$$

we have

$$\chi(\phi^{\boldsymbol{x}}_{\boldsymbol{P}}(\boldsymbol{z})) = \sum_{\boldsymbol{k}\in\mathbb{Z}^n} \hat{\chi}_{\boldsymbol{k}} e^{i\boldsymbol{k}^T(z_1+\boldsymbol{p}_1^T\boldsymbol{x},\ldots,z_n+\boldsymbol{p}_n^T\boldsymbol{x})} = \sum_{\boldsymbol{k}\in\mathbb{Z}^n} \hat{\chi}_{\boldsymbol{k}} e^{i\boldsymbol{k}^T(\boldsymbol{p}_1^T\boldsymbol{x},\ldots,\boldsymbol{p}_n^T\boldsymbol{x})} e^{i\boldsymbol{k}^T\boldsymbol{z}}.$$

Due to the $\phi^{\boldsymbol{x}}_{\boldsymbol{P}}$-invariance of χ and the uniqueness of Fourier coefficients $\hat{\chi}_{\boldsymbol{k}}$, we can obtain

$$\hat{\chi}_{\boldsymbol{k}} = \hat{\chi}_{\boldsymbol{k}} e^{i\boldsymbol{k}^T(\boldsymbol{p}_1^T\boldsymbol{x},\ldots,\boldsymbol{p}_n^T\boldsymbol{x})};$$

i.e.,

$$\hat{\chi}_{\boldsymbol{k}}(1-e^{i\boldsymbol{k}^T(\boldsymbol{p}_1^T\boldsymbol{x},\ldots,\boldsymbol{p}_n^T\boldsymbol{x})})=0.$$

This means that $\hat{\chi}_{\boldsymbol{k}}=0$ or

$$\boldsymbol{k}^T(\boldsymbol{p}_1^T\boldsymbol{x},\ldots,\boldsymbol{p}_n^T\boldsymbol{x})=(\boldsymbol{P}\boldsymbol{k})^T\boldsymbol{x}:=m\in 2\pi\mathbb{Z}. \tag{4.4}$$

Since $\boldsymbol{p}_1,\ldots,\boldsymbol{p}_n$ are rationally independent, then for $\boldsymbol{k}\neq\boldsymbol{0}$ and $m\in 2\pi\mathbb{Z}$, the solution $\boldsymbol{x}$ of (4.4) is countable at most. Obviously, there exists $\boldsymbol{x}_0\in\mathbb{R}^d$ such that $(\boldsymbol{P}\boldsymbol{k})^T\boldsymbol{x}_0\notin 2\pi\mathbb{Z}$ is true for $\boldsymbol{k}\neq\boldsymbol{0}$; then $\hat{\chi}_{\boldsymbol{k}}=0$. Therefore, χ is a constant outside of a set measure zero, which means that $\phi_{\boldsymbol{P}}^{\boldsymbol{x}}$ is ergodic from Lemma 4.1. ∎

The proof of Theorem 4.1 is as follows.

Proof. From the definitions of $\hat{f}_{\boldsymbol{k}}$ and $\hat{F}_{\boldsymbol{k}}$, (4.1) is equivalent to

$$⨍ e^{-i\boldsymbol{\lambda}_{\boldsymbol{k}}^T\boldsymbol{x}}f(\boldsymbol{x})\,d\boldsymbol{x}=\frac{1}{|\mathbb{T}^n|}\int_{\mathbb{T}^n}e^{-i\boldsymbol{k}^T\boldsymbol{y}}F(\boldsymbol{y})\,d\boldsymbol{y};$$

i.e., we need to prove that

$$⨍ e^{-i(\boldsymbol{P}\boldsymbol{k})^T\boldsymbol{x}}F(\boldsymbol{P}^T\boldsymbol{x})\,d\boldsymbol{x}=\frac{1}{|\mathbb{T}^n|}\int_{\mathbb{T}^n}e^{-i\boldsymbol{k}^T\boldsymbol{y}}F(\boldsymbol{y})\,d\boldsymbol{y}. \tag{4.5}$$

Denote $G(\boldsymbol{y})=e^{-i\boldsymbol{k}^T\boldsymbol{y}}F(\boldsymbol{y})$. Equation (4.5) can be rewritten as

$$⨍ G(\boldsymbol{P}^T\boldsymbol{x})\,d\boldsymbol{x}=\frac{1}{|\mathbb{T}^n|}\int_{\mathbb{T}^n}G(\boldsymbol{y})\,d\boldsymbol{y}. \tag{4.6}$$

According to the parameterized translation $\phi_{\boldsymbol{P}}^{\boldsymbol{x}}$ defined in (4.2), (4.6) is equivalent to

$$⨍ G(\phi_{\boldsymbol{P}}^{\boldsymbol{x}}(\boldsymbol{0}))\,d\boldsymbol{x}=\frac{1}{|\mathbb{T}^n|}\int_{\mathbb{T}^n}G(\boldsymbol{y})\,d\boldsymbol{y}. \tag{4.7}$$

Applying the ergodicity of $\phi_{\boldsymbol{P}}^{\boldsymbol{x}}$ proved in Proposition 4.2 and Theorem 4.4, (4.7) is true. The proof of Theorem 4.1 is completed. ∎

We take a one-dimensional quasiperiodic function as an example to demonstrate Theorem 4.1, which can be embedded into a two-dimensional periodic system, as shown in Figure 1. In Figure 1(a), we lift the definition area (blue line) of a one-dimensional quasiperiodic function to two-dimensional periodic lattice as an irrational line by a projection matrix $\boldsymbol{P}=(1,\sqrt{3})$. Then, the irrational line can be reduced to a two-dimensional unit cell by modulo arithmetic due to the two-dimensional periodicity, as shown in Figure 1(b) and Figure 1(c). The irrational slice is infinite, and these moduled lines become dense in the two-dimensional unit cell. Therefore, as Theorem 4.1 states, the one-dimensional quasiperiodic Fourier coefficient can be replaced by the two-dimensional parent Fourier coefficient.

Applying Theorem 4.1, we have the following two corollaries.

Corollary 4.3. *The quasiperiodic function $f(\boldsymbol{x})$ and its parent function are uniquely determined by each other when the projection matrix $\boldsymbol{P}$ is given.*

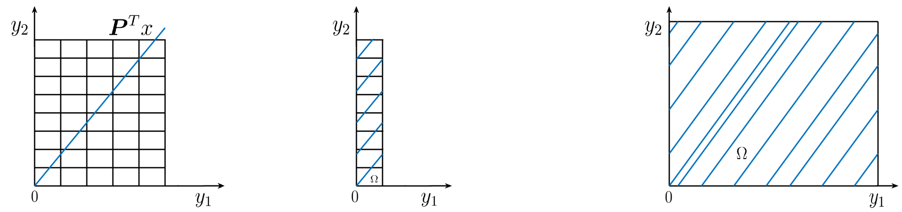

(a) The line $\boldsymbol{P}^T x$ embedded in a two-dimensional periodic lattice

(b) Step 1: Modulo $\boldsymbol{P}^T x$ along y_1-axis

(c) Step 2: Modulo $\boldsymbol{P}^T x$ along y_2-axis after Step 1

FIG. 1. *The process of modulo a two-dimensional irrational slice $\boldsymbol{P}^T x$, where $\boldsymbol{P} = (1, \sqrt{3})$, $x \in \mathbb{R}$.*

Proof. On one hand, when the parent function and the projection matrix $\boldsymbol{P}$ are given, the quasiperiodic function $f(\boldsymbol{x})$ is obviously unique.

On the other hand, we prove that, when the projection matrix $\boldsymbol{P}$ is given, $f(\boldsymbol{x})$ has a unique parent function. Assume that there exist two distinct parent functions $F(\boldsymbol{y})$ and $G(\boldsymbol{y})$ such that

$$f(\boldsymbol{x}) = F(\boldsymbol{P}^T \boldsymbol{x}), \ f(\boldsymbol{x}) = G(\boldsymbol{P}^T \boldsymbol{x}).$$

From Theorem 4.1, we can obtain $\hat{F}_{\boldsymbol{k}} = \hat{f}_{\boldsymbol{k}} = \hat{G}_{\boldsymbol{k}}$, $\boldsymbol{k} \in \mathbb{Z}^n$, where $\hat{F}_{\boldsymbol{k}}$ and $\hat{G}_{\boldsymbol{k}}$ are obtained by the continuous Fourier–Bohr transform, respectively. According to the uniqueness theorem [9], then it follows that $F(\boldsymbol{y}) \equiv G(\boldsymbol{y})$. ∎

Note that the uniqueness theorem in Bohr's work states that the quasiperiodic function is uniquely determined by quasiperiodic Fourier coefficients, which are obtained by the continuous Fourier–Bohr transform [7]. In contrast, Corollary 4.3 states the uniqueness property that arises from the relation between the quasiperiodic function and its parent function.

Furthermore, we can establish an isomorphism relation between a quasiperiodic function space and its parent function space. Denote

$$\mathrm{Tri}(\mathbb{T}^n) = \left\{ F(\boldsymbol{y}) = \sum_{\boldsymbol{k} \in \mathbb{Z}^n} \hat{c}_{\boldsymbol{k}} e^{i \boldsymbol{k}^T \boldsymbol{y}}, \ \boldsymbol{y} \in \mathbb{T}^n : \sum_{\boldsymbol{k} \in \mathbb{Z}^n} |\hat{c}_{\boldsymbol{k}}| < \infty \right\}.$$

For a given projection matrix $\boldsymbol{P} \in \mathbb{M}^{d \times n}$, we define the subspace of $\mathrm{QP}(\mathbb{R}^d)$

$$W_{\boldsymbol{P}}(\mathbb{R}^d) = \{ f(\boldsymbol{x}) \in \mathbb{C}(\mathbb{R}^d) : f(\boldsymbol{x}) = F(\boldsymbol{P}^T \boldsymbol{x}), \ F \in \mathrm{Tri}(\mathbb{T}^n), \ \boldsymbol{P} \in \mathbb{M}^{d \times n} \}.$$

Define a mapping $\varphi_{\boldsymbol{P}} : \mathrm{Tri}(\mathbb{T}^n) \mapsto W_{\boldsymbol{P}}(\mathbb{R}^d)$; then we can easily prove that $\varphi_{\boldsymbol{P}}$ is isomorphic from Corollary 4.3.

COROLLARY 4.4. *For a given function $f(\boldsymbol{x}) \in QP(\mathbb{R}^d)$, where $F(\boldsymbol{y})$ is its parent function, we have the following properties:*

(i) $F(\boldsymbol{y}) \in L^\infty(\mathbb{T}^n)$ *if and only if* $f(\boldsymbol{x}) \in QP_1(\mathbb{R}^d)$.

(ii) $F(\boldsymbol{y}) \in L^2(\mathbb{T}^n)$ *if and only if* $f(\boldsymbol{x}) \in QP_2(\mathbb{R}^d)$.

Proof. For $f(\boldsymbol{x}) \in \mathrm{QP}_1(\mathbb{R}^d)$, we have $f(\boldsymbol{x}) = \sum_{\boldsymbol{k}\in\mathbb{Z}^n} \hat{f}_{\boldsymbol{k}} e^{i(\boldsymbol{P}\boldsymbol{k})^T\boldsymbol{x}}$. Denote the periodic function $g(\boldsymbol{y}) = \sum_{\boldsymbol{k}\in\mathbb{Z}^n} \hat{f}_{\boldsymbol{k}} e^{i\boldsymbol{k}^T\boldsymbol{y}}$. Obviously, $f(\boldsymbol{x}) = g(\boldsymbol{P}^T\boldsymbol{x})$; i.e., $g(\boldsymbol{y})$ is the parent function of $f(\boldsymbol{x})$. Applying Corollary 4.3 and Theorem 4.1 leads to

$$F(\boldsymbol{y}) = g(\boldsymbol{y}) = \sum_{\boldsymbol{k}\in\mathbb{Z}^n} \hat{F}_{\boldsymbol{k}} e^{i\boldsymbol{k}^T\boldsymbol{y}}. \tag{4.8}$$

The Fourier coefficient $\hat{F}_{\boldsymbol{k}}$ is calculated by (2.5), and the Fourier series of the parent function $F(\boldsymbol{y})$ is convergent; i.e., $F(\boldsymbol{y}) \in L^\infty(\mathbb{T}^n)$. Similarly, we can prove that conclusion (i) is sufficient. Conclusion (ii) can be proved similarly. ∎

Applying Parseval's equality (2.4) and Corollary 4.4, for any $F_1,\ F_2 \in \mathrm{Tri}(\mathbb{T}^n)$ and $f_1,\ f_2 \in W_{\boldsymbol{P}}(\mathbb{R}^d)$, we have

$$\|F\|_{L^2}^2 = \sum_{\boldsymbol{k}\in\mathbb{Z}^n} |\hat{c}_{\boldsymbol{k}}|^2, \ \ \|f\|_{\mathcal{L}^2(\mathbb{R}^d)}^2 = \sum_{\boldsymbol{k}\in\mathbb{Z}^n} |\hat{c}_{\boldsymbol{k}}|^2.$$

Therefore, $\|f\|_{\mathcal{L}^2(\mathbb{R}^d)} = \|\varphi_{\boldsymbol{P}} F\|_{\mathcal{L}^2(\mathbb{R}^d)} = \|F\|_{L^2}$; i.e., $\varphi_{\boldsymbol{P}}$ is an isometric mapping in the sense of $\mathcal{L}^2(\mathbb{R}^d)$. The isomorphic mapping $\varphi_{\boldsymbol{P}}$ is a useful tool for error estimates of QSM and PM; see Theorem 5.1 and Theorem 5.3, respectively.

5. Error estimate.

5.1. Error analysis of the QSM. The error analysis of the QSM is built on the relation between the quasiperiodic function and its parent function. Therefore, we first give the truncation error of the periodic Fourier spectral method [21].

LEMMA 5.1. *For each $F \in H^\alpha(\mathbb{T}^n)$, there exists a constant C, independent of F and N, such that*

$$\|\mathcal{P}_N F - F\|_{L^2} \leq C N^{\mu-\alpha} |F|_\alpha.$$

In the following, we will state the error estimate of the QSM in $\mathcal{L}^2(\mathbb{R}^d)$- and $\mathcal{L}^\infty(\mathbb{R}^d)$-norm sense, respectively.

THEOREM 5.1. *Suppose that $f(\boldsymbol{x}) \in QP(\mathbb{R}^d)$ and that its parent function $F(\boldsymbol{y}) \in H^\alpha(\mathbb{T}^n)$ with $\alpha \geq 0$. Then, there exists a constant C, independent of F and N, such that*

$$\|\mathcal{P}_N f - f\|_{\mathcal{L}^2(\mathbb{R}^d)} \leq C N^{-\alpha} |F|_\alpha.$$

Proof. Obviously, Corollary 4.4 implies that $f \in \mathrm{QP}_2(\mathbb{R}^d)$. Since the mapping $\varphi_{\boldsymbol{P}}$ is isometric in the sense of $\mathcal{L}^2(\mathbb{R}^d)$, from Lemma 5.1, we have

$$\begin{aligned}\|\mathcal{P}_N f - f\|_{\mathcal{L}^2(\mathbb{R}^d)} &= \|\mathcal{P}_N \varphi_{\boldsymbol{P}} F - \varphi_{\boldsymbol{P}} F\|_{\mathcal{L}^2(\mathbb{R}^d)} = \|\varphi_{\boldsymbol{P}} \mathcal{P}_N F - \varphi_{\boldsymbol{P}} F\|_{\mathcal{L}^2(\mathbb{R}^d)} \\ &= \|\mathcal{P}_N F - F\|_{L^2} \leq C N^{-\alpha} |F|_\alpha.\end{aligned}$$

This completes the proof. ∎

Another way of proving Theorem 5.1 is presented in Appendix A.

THEOREM 5.2. *Suppose that $f(\boldsymbol{x}) \in QP_1(\mathbb{R}^d)$ and that its parent function $F(\boldsymbol{y}) \in H^\alpha(\mathbb{T}^n)$ with $\alpha > q > n/2$. There exists a constant C_t, independent of F and N, such that*

$$\|\mathcal{P}_N f - f\|_{\mathcal{L}^\infty(\mathbb{R}^d)} \leq C_t N^{q-\alpha} |F|_\alpha.$$

Proof. Applying Theorem 4.1 and the Cauchy–Schwarz inequality, we obtain

$$
\begin{aligned}
\|\mathcal{P}_N f - f\|_{\mathcal{L}^\infty(\mathbb{R}^d)} &= \sup_{\boldsymbol{x}\in\mathbb{R}^n} \left| \sum_{\boldsymbol{k}\in\mathbb{Z}^n/K_N^n} \hat{f}_{\boldsymbol{k}} e^{i(\boldsymbol{P}\boldsymbol{k})^T\boldsymbol{x}} \right| \le \sum_{\boldsymbol{k}\in\mathbb{Z}^n/K_N^n} |\hat{f}_{\boldsymbol{k}}| \\
&\le \left(\sum_{\boldsymbol{k}\in\mathbb{Z}^n/K_N^n} (1+\|\boldsymbol{k}\|_2^2)^{-q} \right)^{1/2} \left(\sum_{\boldsymbol{k}\in\mathbb{Z}^n/K_N^n} (1+\|\boldsymbol{k}\|_2^2)^{q} |\hat{f}_{\boldsymbol{k}}|^2 \right)^{1/2} \\
&\le CN^{q-\alpha} \left(\sum_{\boldsymbol{k}\in\mathbb{Z}^n/K_N^n} (1+\|\boldsymbol{k}\|_2^2)^{-q} \right)^{1/2} \left(\sum_{\boldsymbol{k}\in\mathbb{Z}^n/K_N^n} \|\boldsymbol{k}\|_2^{2\alpha-2q} \cdot (1+\|\boldsymbol{k}\|_2^2)^{q} |\hat{f}_{\boldsymbol{k}}|^2 \right)^{1/2} \\
&\le C2^{q/2}N^{q-\alpha} \left(\sum_{\boldsymbol{k}\in\mathbb{Z}^n/K_N^n} (1+\|\boldsymbol{k}\|_2^2)^{-q} \right)^{1/2} \left(\sum_{\boldsymbol{k}\in\mathbb{Z}^n} \|\boldsymbol{k}\|_2^{2\alpha} \cdot |\hat{f}_{\boldsymbol{k}}|^2 \right)^{1/2} \\
&= C2^{q/2}N^{q-\alpha} \left(\sum_{\boldsymbol{k}\in\mathbb{Z}^n/K_N^n} (1+\|\boldsymbol{k}\|_2^2)^{-q} \right)^{1/2} \left(\sum_{\boldsymbol{k}\in\mathbb{Z}^n} \|\boldsymbol{k}\|_2^{2\alpha} \cdot |\hat{F}_{\boldsymbol{k}}|^2 \right)^{1/2} \\
&\le C_t N^{q-\alpha} |F|_\alpha.
\end{aligned}
$$

The last inequality holds due to $\sum_{\boldsymbol{k}\in\mathbb{Z}^n/K_N^n}(1+\|\boldsymbol{k}\|_2^2)^{-q} < \infty$ when $q > n/2$. ∎

Besides, we can also directly give the error analysis of the QSM without using the parent function; see Appendix B for details. These results also show that the QSM has an exponential convergence rate.

5.2. Error analysis of the PM. The PM grasps the essence that the quasiperiodic function can be embedded into its parent function. Assume that the Fourier series in (4.8) converges to $F(\boldsymbol{y})$ at every grid point of $\mathbb{T}_N^n$. Applying the discrete orthogonality (3.3), the discrete parent Fourier coefficient of (3.4) becomes

$$
(5.1)\quad \tilde{F}_{\boldsymbol{k}} = \langle F, e^{i\boldsymbol{k}^T\boldsymbol{y_j}} \rangle_N = \left\langle \sum_{\boldsymbol{\ell}\in\mathbb{Z}^n} \hat{F}_{\boldsymbol{\ell}} e^{i\boldsymbol{\ell}^T\boldsymbol{y_j}}, e^{i\boldsymbol{k}^T\boldsymbol{y_j}} \right\rangle_N = \hat{F}_{\boldsymbol{k}} + \sum_{\boldsymbol{m}\in\mathbb{Z}_*^n} \hat{F}_{\boldsymbol{k}+2N\boldsymbol{m}},\ \boldsymbol{k}\in K_N^n,
$$

where $\mathbb{Z}_*^n = \mathbb{Z}^n/\{\boldsymbol{0}\}$. Recall that $\boldsymbol{\lambda_k} = \boldsymbol{P}\boldsymbol{k}$, and from (5.1), we have

$$
\sum_{\boldsymbol{k}\in K_N^n} \tilde{F}_{\boldsymbol{k}} e^{i\boldsymbol{\lambda}_{\boldsymbol{k}}^T\boldsymbol{x}} = \sum_{\boldsymbol{k}\in K_N^n} \hat{F}_{\boldsymbol{k}} e^{i\boldsymbol{\lambda}_{\boldsymbol{k}}^T\boldsymbol{x}} + \sum_{\boldsymbol{k}\in K_N^n} \left(\sum_{\boldsymbol{m}\in\mathbb{Z}_*^n} \hat{F}_{\boldsymbol{k}+2N\boldsymbol{m}} \right) e^{i\boldsymbol{\lambda}_{\boldsymbol{k}}^T\boldsymbol{x}}.
$$

From Theorem 4.1 and (3.6), we obtain

$$
\sum_{\boldsymbol{\lambda_k}\in\boldsymbol{\Lambda}_N^d} \tilde{f}_{\boldsymbol{k}} e^{i\boldsymbol{\lambda}_{\boldsymbol{k}}^T\boldsymbol{x}} = \sum_{\boldsymbol{\lambda_k}\in\boldsymbol{\Lambda}_N^d} \hat{f}_{\boldsymbol{k}} e^{i\boldsymbol{\lambda}_{\boldsymbol{k}}^T\boldsymbol{x}} + \sum_{\boldsymbol{\lambda_k}\in\boldsymbol{\Lambda}_N^d} \left(\sum_{\boldsymbol{m}\in\mathbb{Z}_*^n} \hat{f}_{\boldsymbol{k}+2N\boldsymbol{m}} \right) e^{i\boldsymbol{\lambda}_{\boldsymbol{k}}^T\boldsymbol{x}}.
$$

It follows that

$$
I_N f = \mathcal{P}_N f + R_N f,
$$

where

$$
\mathcal{P}_N f = \sum_{\boldsymbol{\lambda_k}\in\boldsymbol{\Lambda}_N^d} \hat{f}_{\boldsymbol{k}} e^{i\boldsymbol{\lambda}_{\boldsymbol{k}}^T\boldsymbol{x}},\ R_N f = \sum_{\boldsymbol{\lambda_k}\in\boldsymbol{\Lambda}_N^d} \left(\sum_{\boldsymbol{m}\in\mathbb{Z}_*^n} \hat{f}_{\boldsymbol{k}+2N\boldsymbol{m}} \right) e^{i\boldsymbol{\lambda}_{\boldsymbol{k}}^T\boldsymbol{x}}.
$$

Similar to the periodic Fourier pseudospectral method, $I_N f$ and $R_N f$ represent the interpolation and the aliasing part, respectively. As a consequence, we have

$$f - I_N f = (f - \mathcal{P}_N f) - R_N f.$$

Thus, the approximation error of PM consists of two parts: the truncation error $f - \mathcal{P}_N f$ as the QSM has and the aliasing error $R_N f$. The truncation error estimates of Theorems 5.1 and 5.2 for QSM are also valid for PM. The aliasing error will be analyzed in the following content. The $\mathcal{L}^2(\mathbb{R}^d)$- and $\mathcal{L}^\infty(\mathbb{R}^d)$-estimates of the interpolation error $f - I_N f$ are stated as follows, respectively.

THEOREM 5.3. *Suppose that $f(\boldsymbol{x}) \in QP(\mathbb{R}^d)$ and that its parent function $F(\boldsymbol{y}) \in H^\alpha(\mathbb{T}^n)$ with $\alpha \geq 0$. There exists a constant C, independent of F and N, such that*

$$\|I_N f - f\|_{\mathcal{L}^2(\mathbb{R}^d)} \leq C N^{-\alpha} |F|_\alpha.$$

Proof. Corollary 4.4 tells us that $f \in \mathrm{QP}_2(\mathbb{R}^d)$. Since $\varphi_{\boldsymbol{P}}(\mathcal{P}_N F) = \mathcal{P}_N(\varphi_{\boldsymbol{P}} F)$ and $\varphi_{\boldsymbol{P}}(R_N F) = R_N(\varphi_{\boldsymbol{P}} F)$, we obtain

$$\begin{aligned}
\|I_N f - f\|_{\mathcal{L}^2(\mathbb{R}^d)} &\leq \|f - \mathcal{P}_N f\|_{\mathcal{L}^2(\mathbb{R}^d)} + \|R_N f\|_{\mathcal{L}^2(\mathbb{R}^d)} \\
&= \|\varphi_{\boldsymbol{P}} F - \mathcal{P}_N(\varphi_{\boldsymbol{P}} F)\|_{\mathcal{L}^2(\mathbb{R}^d)} + \|R_N(\varphi_{\boldsymbol{P}} F)\|_{\mathcal{L}^2(\mathbb{R}^d)} \\
&= \|\varphi_{\boldsymbol{P}} F - \varphi_{\boldsymbol{P}}(\mathcal{P}_N F)\|_{\mathcal{L}^2(\mathbb{R}^d)} + \|\varphi_{\boldsymbol{P}}(R_N F)\|_{\mathcal{L}^2(\mathbb{R}^d)} \\
&= \|F - \mathcal{P}_N F\|_{L^2} + \|R_N F\|_{L^2}.
\end{aligned}$$

Reference [21] (see its section 5.1.3) shows that

$$\|R_N F\|_{L^2} \leq C_1 N^{-\alpha} |F|_\alpha,$$

where C_1 is independent of F and N. Then, the proof is completed by combining Lemma 5.1. ∎

Another way of proving Theorem 5.3 is provided in Appendix C.

THEOREM 5.4. *Suppose that $f(\boldsymbol{x}) \in QP_1(\mathbb{R}^d)$ and that its parent function $F(\boldsymbol{y}) \in H^\alpha(\mathbb{T}^n)$ with $\alpha > q > n/2$. There exists a constant C_p, independent of F and N, such that*

$$\|I_N f - f\|_{\mathcal{L}^\infty(\mathbb{R}^d)} \leq C_p N^{q-\alpha} |F|_\alpha.$$

Proof. According to the definition of $\|\cdot\|_{\mathcal{L}^\infty(\mathbb{R}^d)}$, we have

$$\|I_N f - f\|_{\mathcal{L}^\infty(\mathbb{R}^d)} \leq \sum_{\boldsymbol{\lambda_k} \in \boldsymbol{\Lambda}/\boldsymbol{\Lambda}_N^d} |\hat{f}_{\boldsymbol{k}}| + \sum_{\boldsymbol{\lambda_k} \in \boldsymbol{\Lambda}_N^d} \left| \sum_{\boldsymbol{m} \in \mathbb{Z}_*^n} \hat{f}_{\boldsymbol{k}+2N\boldsymbol{m}} \right|. \tag{5.2}$$

From Theorem 5.2, it follows that

$$\sum_{\boldsymbol{\lambda_k} \in \boldsymbol{\Lambda}/\boldsymbol{\Lambda}_N^d} |\hat{f}_{\boldsymbol{k}}| \leq C_t N^{q-\alpha} |f|_\alpha,$$

where $\alpha > q > n/2$. For the second term on the right side of inequality (5.2), combining it with the Cauchy–Schwarz inequality, we can obtain

$$\begin{aligned}
&\sum_{\boldsymbol{\lambda_k} \in \boldsymbol{\Lambda}_N^d} \left| \sum_{\boldsymbol{m} \in \mathbb{Z}_*^n} \hat{f}_{\boldsymbol{k}+2N\boldsymbol{m}} \right| = \sum_{\boldsymbol{k} \in K_N^n} \left| \sum_{\boldsymbol{m} \in \mathbb{Z}_*^n} \hat{F}_{\boldsymbol{k}+2N\boldsymbol{m}} \right| \leq \sum_{\boldsymbol{k} \in K_N^n} \sum_{\boldsymbol{m} \in \mathbb{Z}_*^n} \left| \hat{F}_{\boldsymbol{k}+2N\boldsymbol{m}} \right| \\
&\quad \leq \left[\sum_{\boldsymbol{k} \in K_N^n} \sum_{\boldsymbol{m} \in \mathbb{Z}_*^n} (1 + \|\boldsymbol{k}+2N\boldsymbol{m}\|_2^2)^{-\alpha} \right]^{\frac{1}{2}} \cdot \left[\sum_{\boldsymbol{k} \in K_N^n} \sum_{\boldsymbol{m} \in \mathbb{Z}_*^n} (1 + \|\boldsymbol{k}+2N\boldsymbol{m}\|_2^2)^{\alpha} |\hat{F}_{\boldsymbol{k}+2N\boldsymbol{m}}|^2 \right]^{\frac{1}{2}}.
\end{aligned}$$

For $\boldsymbol{k} \in K_N^n$ and $\boldsymbol{m} \in \mathbb{Z}_*^n$, we have $\|\boldsymbol{k}+2N\boldsymbol{m}\|_2^2 \geq N^2$. Furthermore, for $\alpha > q$, it follows that

$$\begin{aligned}
&\left[\sum_{\boldsymbol{k}\in K_N^n}\sum_{\boldsymbol{m}\in\mathbb{Z}_*^n}(1+\|\boldsymbol{k}+2N\boldsymbol{m}\|_2^2)^{-\alpha}\right]^{\frac{1}{2}} \\
&\quad = \left[\sum_{\boldsymbol{k}\in K_N^n}\sum_{\boldsymbol{m}\in\mathbb{Z}_*^n}(1+\|\boldsymbol{k}+2N\boldsymbol{m}\|_2^2)^{q-\alpha}\cdot(1+\|\boldsymbol{k}+2N\boldsymbol{m}\|_2^2)^{-q}\right]^{\frac{1}{2}} \\
&\quad = (1+N^2)^{\frac{q-\alpha}{2}}\cdot\left[\sum_{\boldsymbol{k}\in K_N^n}\sum_{\boldsymbol{m}\in\mathbb{Z}_*^n}(1+\|\boldsymbol{k}+2N\boldsymbol{m}\|_2^2)^{-q}\right]^{\frac{1}{2}} \\
&\quad \leq 2^{\frac{q-\alpha}{2}}N^{q-\alpha}\cdot\left[\sum_{\boldsymbol{k}\in K_N^n}\sum_{\boldsymbol{m}\in\mathbb{Z}_*^n}(1+\|\boldsymbol{k}+2N\boldsymbol{m}\|_2^2)^{-q}\right]^{\frac{1}{2}}.
\end{aligned}$$

When $q > n/2$, the series $S := \sum_{\boldsymbol{k}\in K_N^n}\sum_{\boldsymbol{m}\in\mathbb{Z}_*^n}(1+\|\boldsymbol{k}+2N\boldsymbol{m}\|_2^2)^{-q}$ converges. Therefore,

$$\begin{aligned}
&\sum_{\boldsymbol{\lambda}_{\boldsymbol{k}}\in\boldsymbol{\Lambda}_N^d}\left|\sum_{\boldsymbol{m}\in\mathbb{Z}_*^n}\hat{f}_{\boldsymbol{k}+2N\boldsymbol{m}}\right| \\
&\quad \leq 2^{\frac{q-\alpha}{2}}N^{q-\alpha}S^{1/2}\cdot\left[\sum_{\boldsymbol{k}\in K_N^n}\sum_{\boldsymbol{m}\in\mathbb{Z}_*^n}(1+\|\boldsymbol{k}+2N\boldsymbol{m}\|_2^2)^{\alpha}\,|\hat{F}_{\boldsymbol{k}+2N\boldsymbol{m}}|^2\right]^{\frac{1}{2}} \\
&\quad \leq 2^{q/2}N^{q-\alpha}S^{1/2}|F|_\alpha = C_aN^{q-\alpha}|F|_\alpha.
\end{aligned}$$

Then,

$$\|I_Nf-f\|_{\mathcal{L}^\infty(\mathbb{R}^d)} \leq C_tN^{q-\alpha}|F|_\alpha + C_aN^{q-\alpha}|F|_\alpha = C_pN^{q-\alpha}|F|_\alpha.$$

∎

6. Application.

In section 5, we have provided prior estimates of the PM and QSM. In this section, we further investigate the accuracy and efficiency of numerical methods for solving the quasiperiodic system. The TQSE with a spatially quasiperiodic solution is an important quasiperiodic system [16, 30, 31, 32]. Concretely, consider

$$i\psi_t(x,t) = -\frac{1}{2}\psi_{xx}(x,t)+v(x)\psi(x,t),\ \ (x,t)\in\mathbb{R}\times[0,T], \tag{6.1}$$

with incommensurate potential $v(x) = \sum_{\lambda\in\Lambda_1}\hat{v}_\lambda e^{i\lambda x}$, where $\Lambda_1 = \{1,-1,\sqrt{5},-\sqrt{5}\}$ and $\hat{v}_\lambda = 1$. Let the initial value $\psi_0(x) = \sum_{\lambda\in\Lambda_2}\hat{c}_\lambda e^{i\lambda x}$, $x\in\mathbb{R}$, with $\Lambda_2 = \{\lambda = m+n\sqrt{5} : m,n\in\mathbb{Z}, -32\leq m,n\leq 31\}$ and $\hat{c}_\lambda = e^{-(|n|+|m|)}$. Therefore, the projection matrix is $\boldsymbol{P} = (1,\sqrt{5})$. The product term of the wave function $\psi(x,t)$ and potential function $v(x)$, a convolution in the reciprocal space, allows us to examine the performance of different methods.

In the following, we employ the QSM, PM, and PAM to discretize (6.1) in the space direction and the second-order operator splitting (OS2) method in the time direction. In each interval $[0,2\pi)$, we use $2N$ discrete points, corresponding to the number of basis functions of the QSM. Here, we are concerned with the accuracy of spatial quasiperiodic solution; therefore, the final time T can be arbitrary. For simplicity, we choose $T = 0.001$. The time step size $\tau = 1 \times 10^{-7}$ ensures that the time truncation error does not affect the spatial approximation error.

6.1. Numerical implementation.

6.1.1. QSM discretization. As subsection 3.1 states, the QSM approximates the wave function $\psi(x,t)$ in a finite-dimensional space

$$\psi(x,t) \approx \mathcal{P}_N \psi(x,t) = \sum_{\lambda \in \mathbf{\Lambda}_N} \hat{\psi}_\lambda(t) e^{i\lambda x}.$$

The quasiperiodic Fourier coefficient $\hat{\psi}_\lambda$ is obtained by the continuous Fourier–Bohr transform (2.2). $\mathbf{\Lambda}_N$ is defined by (3.1) with $d=1$ and $n=2$. $\#(\mathbf{\Lambda}_N) = (2N)^2 := D$. Then, the TQSE (6.1) is discretized as

$$i \sum_{\lambda \in \mathbf{\Lambda}_N} \frac{d\hat{\psi}_\lambda(t)}{dt} e^{i\lambda x} = \frac{1}{2} \sum_{\lambda \in \mathbf{\Lambda}_N} |\lambda|^2 \hat{\psi}_\lambda(t) e^{i\lambda x} + \left(\sum_{\lambda \in \Lambda_1} \hat{v}_\lambda e^{i\lambda x} \right) \left(\sum_{\lambda \in \mathbf{\Lambda}_N} \hat{\psi}_\lambda(t) e^{i\lambda x} \right). \tag{6.2}$$

Making the inner product of (6.2) by $e^{i\beta x}$ and applying the orthogonality (2.1), we obtain

$$i\frac{d\hat{\psi}_\beta(t)}{dt} = \frac{1}{2}|\beta|^2 \hat{\psi}_\beta(t) + \sum_{\lambda \in \mathbf{\Lambda}_N} \hat{v}_{\beta-\lambda} \hat{\psi}_\beta(t), \ \beta \in \mathbf{\Lambda}_N. \tag{6.3}$$

By applying the OS2 method to the semidiscrete equation (6.3), we can obtain the fully discrete scheme as given in Appendix D.1. Since the QSM cannot use an FFT, the computational cost of solving (6.3) in each time step is dominated by the convolution calculation with computational complexity of $O(D^2)$.

6.1.2. PM discretization. The PM is a generalized Fourier pseudospectral method. As a sequence, the PM can further discretize x variable through the collocation points $x_j = \boldsymbol{P}\boldsymbol{y}_j$ with $\boldsymbol{y}_{\boldsymbol{j}} = (j_1\pi/N, j_2\pi/N) \in \mathbb{T}_N^2$, $0 \le j_1, j_2 < 2N$. We can expand the spatial function by discrete Fourier–Bohr expansion

$$\psi(x_j,t) \approx I_N \psi(x_j,t) = \sum_{\boldsymbol{\lambda} \in \mathbf{\Lambda}_N} \tilde{\psi}_\lambda(t) e^{i\lambda x_j} \ \ j = 0, 1, \dots, D-1,$$

where $\tilde{\psi}_\lambda(t) = \tilde{\Psi}_{\boldsymbol{k}}(t) = \langle \Psi, e^{i\boldsymbol{k}^T \boldsymbol{y}_{\boldsymbol{j}}} \rangle_N$, $\lambda = \boldsymbol{P}\boldsymbol{k}$, and $D = (2N)^2$ is the number of spatial nodes.

Denote that $V(\boldsymbol{y})$ is the parent function of $v(x)$. Similarly, we can expand $v(x)$ using the discrete Fourier–Bohr transform. The TQSE (6.1) is discretized as

$$i \sum_{\lambda \in \mathbf{\Lambda}_N} \frac{d\tilde{\psi}_\lambda(t)}{dt} e^{i\lambda x_j} = \frac{1}{2} \sum_{\lambda \in \mathbf{\Lambda}_N} |\lambda|^2 \tilde{\psi}_\lambda(t) e^{i\lambda x_j} + \left(\sum_{\lambda \in \Lambda_1} \tilde{v}_\lambda e^{i\lambda x_j} \right) \left(\sum_{\lambda \in \mathbf{\Lambda}_N} \tilde{\psi}_\lambda(t) e^{i\lambda x_j} \right), \tag{6.4}$$

where $\tilde{v}_\lambda = \langle V, e^{i\boldsymbol{k}^T \boldsymbol{y}_{\boldsymbol{j}}} \rangle_N$. Taking the discrete inner product of (6.4) by $e^{i\beta x_j}$ and applying the discrete orthogonality (3.3) yields

$$i\frac{d\tilde{\psi}_\beta(t)}{dt} = \frac{1}{2}|\beta|^2 \tilde{\psi}_\beta(t) + \sum_{\lambda \in \mathbf{\Lambda}_N} \tilde{v}_{\beta-\lambda} \tilde{\psi}_\lambda(t), \ \beta \in \mathbf{\Lambda}_N. \tag{6.5}$$

Similarly, the OS2 method can be applied to discretize the semidiscrete equation (6.5). The corresponding fully discrete scheme can be found in Appendix D.2. Meanwhile, we can use an FFT to efficiently compute the convolution terms in (6.5) based on the discrete Fourier–Bohr transform. Therefore, the computational complexity of the PM in each time step is the level of $O(D\log D)$.

6.1.3. PAM discretization. The PAM, using a periodic system to approximate the quasiperiodic systems, is a widely used approach to addressing quasiperiodic systems [10]. Here, we use a periodic Schrödinger equation over a finite fundamental region $[0,2\pi L)$, $L\in\mathbb{N}_0$ to approximate the TQSE. Then, we can use the periodic Fourier pseudospectral method to solve the approximated periodic Schrödinger equation. We use $D=2ML$ discrete points to discretize the one-dimensional periodic system. The computational complexity in each time step is at the level of $O((2ML)\log(2ML))$. Appendix D.3 provides the implementation of the PAM of solving the TQSE.

6.2. Numerical results. In this subsection, we present numerical results of solving the TQSE (6.1) by using the PM, QSM, and PAM. All algorithms are coded by MSVC++ 14.29 on Visual Studio Community 2019. The FFT used in the PM and PAM is based on the software FFTW 3.3.5 [33]. All computations are carried out on a workstation with an Intel Core 2.30 GHz CPU, 16 GB RAM. The reference solution $\psi^*(x,T)$ is obtained by using the PM with a time step size $\tau=1\times10^{-7}$, a fine mesh size $h=\pi/128$, and a final time $T=0.001$. In our numerical results, we mainly show the numerical error e_N and CPU time of three algorithms. First, we give the calculation formula of the e_N of the QSM, PM, and PAM. Denote the exact solution of the TQSE

$$\psi^*(x,T)=\sum_{\lambda\in\Lambda}\tilde{\psi}^*_\lambda(T)e^{i\lambda x}.$$

In the QSM, from Parseval's equality, the numerical error is

$$\begin{aligned}
e_N^2 &= \|\psi^*(x,T)-\mathcal{P}_N\psi(x,T)\|^2_{\mathcal{L}^2(\mathbb{R})}\\
&= \lim_{K\to+\infty}\frac{1}{2K}\int_{-K}^{K}|\psi^*(x,T)-\mathcal{P}_N\psi(x,T)|^2\,dx\\
&= \sum_{\lambda\in\Lambda_N}|\tilde{\psi}^*_\lambda(T)-\hat{\psi}_\lambda(T)|^2.
\end{aligned}$$

In the PM, we can obtain

$$e_N^2=\|\psi^*(x,T)-I_N\psi(x,T)\|^2_{\mathcal{L}^2(\mathbb{R})}=\sum_{\lambda\in\Lambda_N}|\tilde{\psi}^*_\lambda(T)-\tilde{\psi}_\lambda(T)|^2.$$

In the PAM, assume that the exact solution of the periodic Schrödinger system (D.5) is

$$\varphi^*(x,T)=\sum_{k\in\mathbb{Z}}\tilde{\psi}^*_k(T)e^{ikx},\ \ x\in[0,2\pi L).$$

The numerical solution obtained by the PAM is

$$\varphi_M(x,T)=\sum_{k\in\Lambda_M^{PAM}}\tilde{\varphi}_k(T)e^{ikx},\ \ x\in[0,2\pi L),$$

where $\Lambda_M^{PAM} = \{k \in \mathbb{Z} : -LM \le k < LM\}$ is a finite subset of $\mathbb{Z}$ containing a subset of $\{k \in \mathbb{Z} : k = [L\lambda], \lambda \in \Lambda_N\}$. Then, we can compute the numerical error

$$e_M^2 = \|\varphi^*(x,T) - \varphi_M(x,T)\|_{L^2([0,2\pi L))} = \sum_{k\in\Lambda_M^{PAM}} |\tilde{\psi}_k^*(T) - \tilde{\varphi}_k(T)|^2.$$

Therefore, the errors of three methods are all measured by the convergence of corresponding Fourier coefficients. Note that both the QSM and PM calculate the global quasiperiodic system over $\mathbb{R}$, while the PAM only computes a periodic approximation system on a fundamental period $[0, 2\pi L)$.

We present the numerical results of the PAM with $M = 4N$. For convenience, we use e_N to replace e_M. Through extensive experiments, we adopt $N = 8$ (also see Table 1) in the PAM to ensure enough numerical accuracy of discretizing TQSE.

Figure 2(a) shows the approximation error obtained by the PAM with $N = 8$. The approximation error e_N of the PAM exhibits an oscillation phenomenon as the domain size L increases. This behavior can be attributed to the Diophantine approximation

TABLE 1
Numerical error e_N of the PM, QSM, and PAM for different N.

N	2	4	8	16	32
PM	4.132e-03	7.569e-04	2.543e-05	1.702e-08	1.748e-12
QSM	4.132e-03	7.569e-04	2.543e-05	1.702e-08	1.903e-12
PAM ($L = 17$)	1.907e-02	1.900e-02	1.899e-02	1.899e-02	1.899e-02
PAM ($L = 72$)	4.536e-03	4.449e-03	4.449e-03	4.449e-03	4.449e-03
PAM ($L = 305$)	1.376e-03	1.052e-03	1.051e-03	1.051e-03	1.051e-03
PAM ($L = 1292$)	9.219e-04	2.529e-04	2.480e-04	2.480e-04	2.480e-04

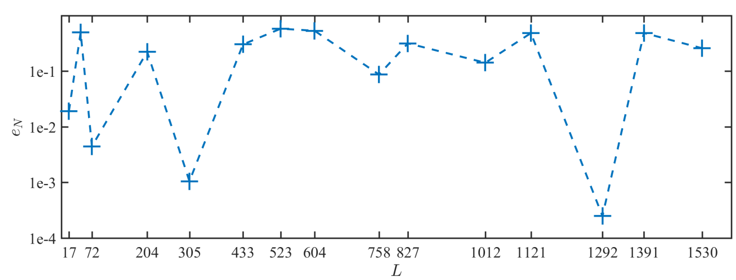

(a) In the PAM, the relationship between the numerical error e_N and L with $N = 8$.

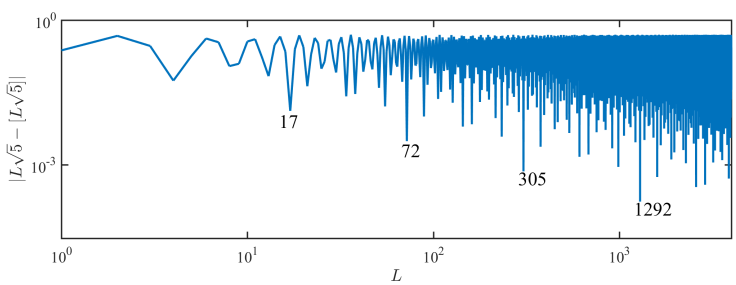

(b) Diophantine approximation error

FIG. 2. *Approximation error of the PAM as the domain size L increases.*

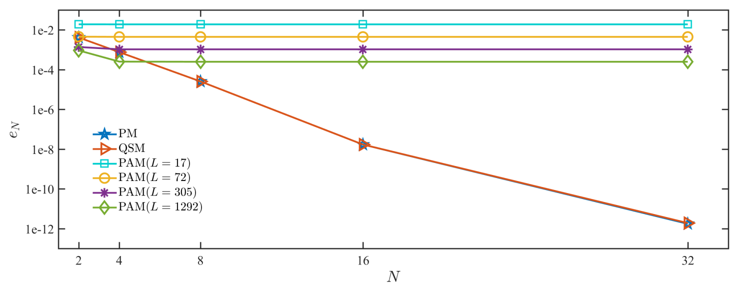

FIG. 3. *The relationship between the numerical error e_N and N.*

error, i.e., using rational numbers to approximate the irrational number. As depicted in Figure 2(b), the Diophantine approximation error $\{L\sqrt{5}\} := |L\sqrt{5} - [L\sqrt{5}]|$, where $[\alpha]$ denotes the nearest integer to α, does not uniformly decrease with an increase of L due to the arithmetic property of irrational number $\sqrt{5}$. The relevant function approximation theory on the PAM can refer to [11]. For specific values of L, such as 17, 72, 305, and 1292, the Diophantine approximation error as well as the approximation error e_N can gradually decrease.

Then, we compare the approximation error e_N of the PM, QSM, and PAM. Table 1 shows the e_N of three algorithms as discrete points increase. Figure 3 gives a visual image to show the convergence rate. For the PAM, we only present these results when $L = 17$, 72, 305, 1292. The approximation error of the PAM consists of the quasiperiodic approximation error determined by the Diophantine approximation error $\{L\sqrt{5}\}$ and the numerical discrete error of solving a periodic Schrödinger system (D.5). The quasipepriodic approximation error is mainly controlled by the Diophantine approximation error. The numerical discrete error is dependent on the discrete points. Once L is fixed, the discrete points achieve a critical value; then the e_N of the PAM cannot decrease, as shown in Table 1. Therefore, the e_N of the PAM is mainly determined by the quasiperiodic approximation error. Theoretically, the e_N of the PAM can decrease by choosing a large and reasonable L. However, the resulting computational cost could be unbearable. More significantly, L cannot go to infinity in the numerical computation. As a result, the quasiperiodic approximation error cannot be avoided. Table 1 also shows that the QSM and PM both have exponentially convergent rates in solving the TQSE, consistent with the error estimates in section 5. Besides, the aliasing error $\|R_N\psi\|_{\mathcal{L}^2(\mathbb{R})}$ of PM is almost smaller than the level of 10^{-12}, even for the 4×4 grid.

We examine the efficiency of three methods by comparing CPU time in solving the TQSE, as shown in Table 2. These results demonstrate that the CPU time required by the QSM increases dramatically with an increase of N due to the invalidity of the FFT. In contrast, the PM can greatly save computational amounts by using an FFT. The CPU time of the PAM has a similar behavior as the PM due to the availability of the FFT. However, the PAM is less efficient than the PM since the PAM needs more discrete nodes.

Finally, combining the data in Table 1 and Table 2, we plot the relationship between e_N and CPU time in Figure 4. These results show that the PM is a high-precision and efficient algorithm in solving the TQSE (6.1).

Table 2
Required CPU time (s) of the PM, QSM, and PAM for different N.

N	2	4	8	16	32
PM	0.051	0.077	0.237	0.716	2.873
QSM	0.125	1.020	13.366	198.301	3347.355
PAM ($L=17$)	0.331	0.593	1.146	2.554	4.204
PAM ($L=72$)	0.994	1.833	3.741	7.382	15.947
PAM ($L=305$)	6.497	12.853	27.451	64.089	109.709
PAM ($L=1292$)	28.625	50.074	114.273	247.594	494.179

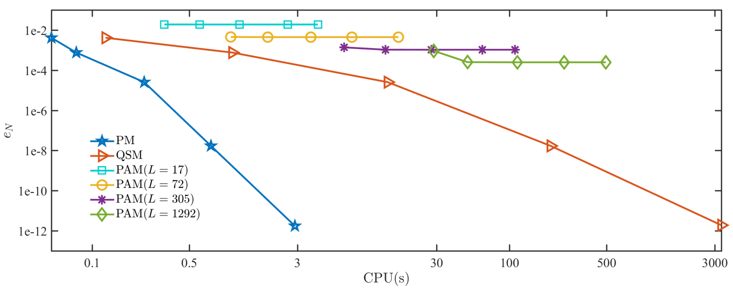

Fig. 4. *The relationship between the numerical error e_N and CPU time (s) when $N = 2, 4, 8, 16, 32$, respectively.*

7. Discussion and conclusions. In this paper, we present the convergence analysis of the PM and QSM by revealing the relation between quasiperiodic functions and their parent functions. These results demonstrate that the PM and QSM have exponential decay both in $\mathcal{L}^2(\mathbb{R}^d)$- and $\mathcal{L}^\infty(\mathbb{R}^d)$-norm and that the QSM (PM) is an extension of the periodic Fourier spectral (pseudospectral) method. We also analyze the computational complexity of these methods. The PM can use an FFT, while the QSM cannot. Finally, we adopt a one-dimensional TQSE to show the accuracy and efficiency of the PM, QSM, and PAM in solving quasiperiodic systems. Numerical results demonstrate that the PM and QSM also have exponential convergence, while the approximation error of the PAM is mainly dominated by the Diophantine approximation error. These results show that the PM is an accurate and efficient method for solving quasiperiodic systems. It is the first theoretical work of the PM. This work encourages us to further investigate the error estimates of the PM and QSM in a general function space, as well as the development of advanced numerical methods and theories for solving more quasiperiodic systems.

Appendix A. The proof of Theorem 5.1.

Proof. For $\boldsymbol{k} \in K_N^n$, it follows that $\|\boldsymbol{k}\|_2 \leq \sqrt{n}N$. By the Cauchy–Schwarz inequality and applying Theorem 4.1, we have

$$\begin{aligned}\|\mathcal{P}_N f - f\|^2_{\mathcal{L}^2(\mathbb{R}^d)} &= \sum_{\boldsymbol{k}\in\mathbb{Z}^n/K_N^n} |\hat{f}_{\boldsymbol{k}}|^2 \leq CN^{-2\alpha} \sum_{\boldsymbol{k}\in\mathbb{Z}^n/K_N^n} \|\boldsymbol{k}\|_2^{2\alpha}|\hat{f}_{\boldsymbol{k}}|^2 \\ &= CN^{-2\alpha} \sum_{\boldsymbol{k}\in\mathbb{Z}^n/K_N^n} \|\boldsymbol{k}\|_2^{2\alpha}|\hat{F}_{\boldsymbol{k}}|^2 \leq CN^{-2\alpha}|F|^2_\alpha.\end{aligned}$$

This completes the proof. ∎

Appendix B. Error analysis of the QSM without the help of parent functions. Here, we present an approximation analysis of the QSM in the quasiperiodic function space by imposing some assumptions on the projection matrix.

THEOREM B.1. *Suppose that $f(\boldsymbol{x}) \in H^{\alpha}_{QP}(\mathbb{R}^d)$ and that the nonzero minimum singular value $\sigma_{\min}(\boldsymbol{P})$ of the projection matrix $\boldsymbol{P}$ satisfies $\sigma_{\min}(\boldsymbol{P}) > \theta > 0$. Then, there exists a constant $C(\theta)$, independent of f and N, such that*

$$\|\mathcal{P}_N f - f\|_{\mathcal{L}^2(\mathbb{R}^d)} \leq C(\theta) N^{-\alpha} |f|_{\alpha}.$$

Proof. For $\boldsymbol{k} \in K_N^n$, it follows that $\|\boldsymbol{k}\|_2 \leq \sqrt{n}N$. By the Cauchy–Schwarz inequality, we have

$$\begin{aligned}\|\mathcal{P}_N f - f\|^2_{\mathcal{L}^2(\mathbb{R}^d)} &= \sum_{\boldsymbol{k}\in\mathbb{Z}^n/K_N^n} |\hat{f}_{\boldsymbol{k}}|^2 = \sum_{\boldsymbol{\lambda}\in\boldsymbol{\Lambda}/\boldsymbol{\Lambda}_N^d} |\hat{f}_{\boldsymbol{\lambda}}|^2 \\ &\leq (\sigma_{\min}(\boldsymbol{P})CN)^{-2\alpha} \sum_{\boldsymbol{\lambda}\in\boldsymbol{\Lambda}/\boldsymbol{\Lambda}_N^d} \|\boldsymbol{\lambda}\|_2^{2\alpha} |\hat{f}_{\boldsymbol{\lambda}}|^2 \leq C(\theta) N^{-2\alpha} |f|^2_{\alpha}.\end{aligned}$$

This completes the proof. ∎

THEOREM B.2. *Suppose that $f(\boldsymbol{x}) \in H^{\alpha}_{QP}(\mathbb{R}^d)$, that the nonzero minimum singular value $\sigma_{\min}(\boldsymbol{P})$ of the projection matrix $\boldsymbol{P}$ satisfies $\sigma_{\min}(\boldsymbol{P}) > \theta > 0$, and that $\alpha > q > d/2$. Then, there exists a constant $C(\theta)$, independent of f and N, such that*

$$\|\mathcal{P}_N f - f\|_{\mathcal{L}^\infty(\mathbb{R}^d)} \leq C(\theta) N^{q-\alpha} |f|_{\alpha}.$$

Proof. Applying the Cauchy–Schwarz inequality, we obtain

$$\begin{aligned}\|\mathcal{P}_N f - f\|_{\mathcal{L}^\infty(\mathbb{R}^d)} &= \sup_{\boldsymbol{x}\in\mathbb{R}^n} \left| \sum_{\boldsymbol{k}\in\mathbb{Z}^n/K_N^n} \hat{f}_{\boldsymbol{k}} e^{i(\boldsymbol{P}\boldsymbol{k})^T\boldsymbol{x}} \right| \leq \sum_{\boldsymbol{k}\in\mathbb{Z}^n/K_N^n} |\hat{f}_{\boldsymbol{k}}| = \sum_{\boldsymbol{\lambda}\in\boldsymbol{\Lambda}/\boldsymbol{\Lambda}_N^d} |\hat{f}_{\boldsymbol{\lambda}}| \\ &\leq \left(\sum_{\boldsymbol{\lambda}\in\boldsymbol{\Lambda}/\boldsymbol{\Lambda}_N^d} \|\boldsymbol{\lambda}\|_2^{-2q} \right)^{1/2} \left(\sum_{\boldsymbol{\lambda}\in\boldsymbol{\Lambda}/\boldsymbol{\Lambda}_N^d} \|\boldsymbol{\lambda}\|_2^{2q} |\hat{f}_{\boldsymbol{\lambda}}|^2 \right)^{1/2} \\ &= \left(\sum_{\boldsymbol{\lambda}\in\boldsymbol{\Lambda}/\boldsymbol{\Lambda}_N^d} \|\boldsymbol{\lambda}\|_2^{-2q} \right)^{1/2} \left(\sum_{\boldsymbol{\lambda}\in\boldsymbol{\Lambda}/\boldsymbol{\Lambda}_N^d} \|\boldsymbol{\lambda}\|_2^{2q-2\alpha} \|\boldsymbol{\lambda}\|_2^{2\alpha} |\hat{f}_{\boldsymbol{\lambda}}|^2 \right)^{1/2} \\ &\leq C[\sigma_{min}(\boldsymbol{P})N]^{q-\alpha} \left(\sum_{\boldsymbol{\lambda}\in\boldsymbol{\Lambda}/\boldsymbol{\Lambda}_N^d} \|\boldsymbol{\lambda}\|_2^{-2q} \right)^{1/2} \left(\sum_{\boldsymbol{\lambda}\in\boldsymbol{\Lambda}/\boldsymbol{\Lambda}_N^d} \|\boldsymbol{\lambda}\|_2^{2\alpha} |\hat{f}_{\boldsymbol{\lambda}}|^2 \right)^{1/2} \\ &\leq C[\sigma_{min}(\boldsymbol{P})N]^{q-\alpha} \left(\sum_{\boldsymbol{\lambda}\in\boldsymbol{\Lambda}/\boldsymbol{\Lambda}_N^d} \|\boldsymbol{\lambda}\|_2^{-2q} \right)^{1/2} \left(\sum_{\boldsymbol{\lambda}\in\boldsymbol{\Lambda}} |\boldsymbol{\lambda}|^{2\alpha} |\hat{f}_{\boldsymbol{\lambda}}|^2 \right)^{1/2} \\ &= C(\theta) N^{q-\alpha} |f|_{\alpha}.\end{aligned}$$

The last inequality holds due to $\sum_{\boldsymbol{\lambda}\in\boldsymbol{\Lambda}/\boldsymbol{\Lambda}_N^d} \|\boldsymbol{\lambda}\|_2^{-2q} < \infty$ when $q > d/2$. ∎

Appendix C. Another proof of Theorem 5.3. According to the definition of $\mathcal{L}^2(\mathbb{R}^d)$-norm, we have

$$\begin{aligned}\|f-I_Nf\|^2_{\mathcal{L}^2(\mathbb{R}^d)} &= \sum_{\boldsymbol{\lambda_k}\in\boldsymbol{\Lambda}/\boldsymbol{\Lambda}_N^d} |\hat{f}_{\boldsymbol{k}}|^2 + \sum_{\boldsymbol{\lambda_k}\in\boldsymbol{\Lambda}_N^d}\left|\sum_{\boldsymbol{m}\in\mathbb{Z}^n_*}\hat{f}_{\boldsymbol{k}+2N\boldsymbol{m}}\right|^2\\ &= \|f-\mathcal{P}_Nf\|^2_{\mathcal{L}^2(\mathbb{R}^d)} + \|R_Nf\|^2_{\mathcal{L}^2(\mathbb{R}^d)}.\end{aligned}$$

Recall that $\|\boldsymbol{k}\|_2^2 = \sum_{j=1}^n |k_j|^2$, and by the Cauchy–Schwarz inequality, we have

$$\begin{aligned}\left|\sum_{\boldsymbol{m}\in\mathbb{Z}^n_*}\hat{f}_{\boldsymbol{k}+2N\boldsymbol{Pm}}\right|^2 &= \left|\sum_{\boldsymbol{m}\in\mathbb{Z}^n_*}\hat{F}_{\boldsymbol{k}+2N\boldsymbol{m}}\right|^2\\ &= \left|\sum_{\boldsymbol{m}\in\mathbb{Z}^n_*}(1+\|\boldsymbol{k}+2N\boldsymbol{m}\|_2^2)^{-\frac{\alpha}{2}}\cdot(1+\|\boldsymbol{k}+2N\boldsymbol{m}\|_2^2)^{\frac{\alpha}{2}}\,\hat{F}_{\boldsymbol{k}+2N\boldsymbol{m}}\right|^2\\ &\le \sum_{\boldsymbol{m}\in\mathbb{Z}^n_*}(1+\|\boldsymbol{k}+2N\boldsymbol{m}\|_2^2)^{-\alpha}\cdot\sum_{\boldsymbol{m}\in\mathbb{Z}^n_*}(1+\|\boldsymbol{k}+2N\boldsymbol{m}\|_2^2)^{\alpha}\,|\hat{F}_{\boldsymbol{k}+2N\boldsymbol{m}}|^2.\end{aligned}$$

Since $|k_j|\le N$, $j=1,\dots,n$, for $|m_j|\ge 1$, it follows that

$$|k_j+2Nm_j| \ge 2N|m_j| - |k_j| \ge (2|m_j|-1)N > 1.$$

Thus, for $\boldsymbol{m}\in\mathbb{Z}^n$ with $|m_j|\ge 1$, we have

$$\begin{aligned}(1+\|\boldsymbol{k}+2N\boldsymbol{m}\|_2^2)^{-\alpha} &= \left[1+\sum_{j=1}^n|k_j+2Nm_j|^2\right]^{-\alpha}\\ &\le \left[1+\sum_{j=1}^n((2|m_j|-1)N)^2\right]^{-\alpha} \le N^{-2\alpha}\left[\sum_{j=1}^n(2|m_j|-1)^2\right]^{-\alpha}.\end{aligned}$$

Then,

$$\sum_{\boldsymbol{m}\in\mathbb{Z}^n_*}(1+\|\boldsymbol{k}+2N\boldsymbol{m}\|_2^2)^{-\alpha} \le N^{-2\alpha}\sum_{r=1}^n 2^r C_n^r \sum_{m_1=1}^{+\infty}\cdots\sum_{m_r=1}^{+\infty}\left[\sum_{j=1}^r(2|m_j|-1)^2\right]^{-\alpha}.$$

When $\alpha > r/2$, the series $\sum_{m_1=1}^{+\infty}\cdots\sum_{m_r=1}^{+\infty}\left[\sum_{j=1}^r(2|m_j|-1)^2\right]^{-\alpha}$ converges. For $\alpha > n/2$, we have

$$S := \sum_{\boldsymbol{m}\in\mathbb{Z}^n_*}\left[\sum_{j=1}^d(2|m_j|-1)\right]^{-\alpha} < \infty.$$

Therefore,

$$\begin{aligned}
\|R_N f\|^2_{\mathcal{L}^2(\mathbb{R}^d)} &= \sum_{\boldsymbol{k}\in K_N^n} \left| \sum_{\boldsymbol{m}\in\mathbb{Z}_*^n} \hat{F}_{\boldsymbol{k}+2N\boldsymbol{m}} \right|^2 \\
&\le N^{-2\alpha} S \cdot \sum_{\boldsymbol{k}\in K_N^n} \sum_{\boldsymbol{m}\in\mathbb{Z}_*^n} (1+\|\boldsymbol{k}+2N\boldsymbol{m}\|_2^2)^\alpha \, |\hat{F}_{\boldsymbol{k}+2N\boldsymbol{m}}|^2 \\
&\le N^{-2\alpha} S \cdot 2^\alpha \sum_{\boldsymbol{k}\in K_N^n} \sum_{\boldsymbol{m}\in\mathbb{Z}_*^n} \|\boldsymbol{k}+2N\boldsymbol{m}\|_2^{2\alpha} \, |\hat{F}_{\boldsymbol{k}+2N\boldsymbol{m}}|^2 \\
&\le 2^\alpha N^{-2\alpha} S |F|_\alpha^2.
\end{aligned}$$

Applying Lemma 5.1 yields

$$\|f - I_N f\|_{\mathcal{L}^2(\mathbb{R}^d)} \le C N^{-\alpha} |F|_\alpha.$$

Appendix D. Fully discrete scheme of the TQSE (6.1). We apply the OS2 method to solving semidiscrete equations (6.3) and (6.5) in the time direction. Meanwhile, we present the implementation details of the PAM to solve the TQSE (6.1). Let τ be the time size, and let the mth time iteration step $t_m = m\tau$.

D.1. Fully discrete scheme using the QSM. From t_m to t_{m+1}, the OS2 scheme consists of three steps to solving (6.3).

Step 1: Consider the following ordinary differential equation for $t \in [t_m, t_m + \tau/2]$,

$$i\frac{d\hat{\psi}_\beta(t)}{dt} = \frac{1}{2}|\beta|^2 \hat{\psi}_\beta(t), \tag{D.1}$$

with initial value $\hat{\psi}_\beta(t_m)$. We can analytically solve (D.1) and obtain

$$\hat{\phi}_\beta(t_m) = \hat{\psi}_\beta\left(t_m + \frac{\tau}{2}\right) = e^{-(i\beta^2\tau)/4} \hat{\psi}_\beta(t_m). \tag{D.2}$$

Step 2: Consider (D.3) for $t \in [t_m, t_{m+1}]$,

$$i\frac{d\hat{\psi}_\beta(t)}{dt} = \sum_{\lambda\in\boldsymbol{\Lambda}_N} \hat{v}_{\beta-\lambda} \hat{\psi}_\lambda(t) := g(t, \hat{\psi}_\beta(t)), \tag{D.3}$$

with initial value $\hat{\phi}_\beta(t_m)$. To address the convolution term, we apply the fourth-order Runge–Kutta (RK4) method to solve (D.3) in the reciprocal space. Concretely, let $k_1 = g(t_m, \hat{\phi}_\beta(t_m))$, $k_2 = g(t_m + \tau/2, \hat{\phi}_\beta(t_m) + \tau k_1/2)$, $k_3 = g(t_m + \tau/2, \hat{\phi}_\beta(t_m) + \tau k_2/2)$, and $k_4 = g(t_m + \tau, \hat{\phi}_\beta(t_m) + \tau k_3)$; then $\hat{\phi}_\beta(t_{m+1}) = \hat{\phi}_\beta(t_m) + \tau(k_1 + 2k_2 + 2k_3 + k_4)/6$.

Step 3: Still consider (D.1), but with initial value $\hat{\phi}_\beta(t_{m+1})$ for $t \in [t_m + \tau/2, t_{m+1}]$; then we can obtain $\hat{\psi}_\beta(t_{m+1})$ analytically.

Here, we analyze the computational complexity for each time step. In Steps 1 and 3, the QSM can analytically solve (D.1), resulting in D multiplication operators, respectively. In Step 2, due to the RK4 scheme and convolution summations, there are $8D^2 + 14D$ operators. Therefore, the computational complexity of the QSM in solving (6.1) is the level of $O(D^2)$.

D.2. Fully discrete scheme using the PM. From t_m to t_{m+1}, the OS2 scheme also contains three steps in solving (6.5). Step 1 and Step 3 are similar to

Appendix D.1. In Step 2, we can calculate the convolution terms of (6.5) by using a two-dimensional FFT; we obtain

$$\Phi(\boldsymbol{y_j}, t_m) = \sum_{\boldsymbol{k}\in K_N^2} \tilde{\Phi}_{\boldsymbol{k}}(t_m) e^{i\boldsymbol{k}^T \boldsymbol{y_j}},$$

where $\tilde{\Phi}_{\boldsymbol{k}}(t_m)$ is obtained by Step 1. Consider the equation for $t \in [t_m, t_{m+1}]$,

$$i\Psi_t = V(\boldsymbol{y_j})\Psi(\boldsymbol{y_j}, t) := w(t, \Psi(\boldsymbol{y_j}, t)), \tag{D.4}$$

where the initial value is $\Phi(\boldsymbol{y_j}, t_m)$ and $V(\boldsymbol{y})$ is the parent function corresponding to $v(x)$. To make a fair comparison with the QSM, we still use the RK4 to solve (D.4) in physical space. Let $k_1 = w(t_m, \Phi(\boldsymbol{y_j}, t_m))$, $k_2 = w(t_m + \tau/2, \Phi(\boldsymbol{y_j}, t_m) + \tau k_1/2)$, $k_3 = w(t_m + \tau/2, \Phi(\boldsymbol{y_j}, t_m) + \tau k_2/2)$, and $k_4 = w(t_m + \tau, \Phi(\boldsymbol{y_j}, t_m) + \tau k_3)$; then $\Phi(\boldsymbol{y_j}, t_{m+1}) = \Phi(\boldsymbol{y_j}, t_m) + \tau(k_1 + 2k_2 + 2k_3 + k_4)/6$. Again using an FFT, we obtain $\tilde{\phi}_\beta(t_{m+1}) = \langle \Phi, e^{i\boldsymbol{k}^T \boldsymbol{y_j}}\rangle_N$.

Next, we analyze the computational complexity of each time step. Similarly, the differential systems in Steps 1 and 3 can be analytically solved in the reciprocal space, resulting in D multiplication operators, respectively. In Step 2, due to the availability of the FFT, the convolutions in (6.5) can be economically calculated in physical space as a dot product as shown in (D.4), which raises $O(D\log D)$ operators. Therefore, the computational complexity of the PM in solving (6.1) is the level of $O(D\log D)$.

D.3. Implementation of the PAM of solving the TQSE (6.1). We give the implementation of the PAM to solve the TQSE (6.1). In the PAM, we use a one-dimensional periodic Schrödinger equation (PSE) to approximate the TQSE (6.1) over a finite region $[0, 2\pi L)$. Concretely, we use the periodic functions $u(x)$ and $\varphi(x,t)$ to approximate $v(x)$ and $\psi(x,t)$, respectively. Denote

$$\Lambda(u) = \{h \in \mathbb{Z} : h = [L\lambda],\ \lambda \in \Lambda_1\};$$

then

$$u(x) = \sum_{h\in\Lambda(u)} \hat{u}_h e^{ihx},\ x \in [0, 2\pi L),$$

where $\hat{u}_h = \hat{u}_{[L\lambda]} = \hat{v}_\lambda = 1$. Therefore, the PAM solves the one-dimensional PSE

$$i\frac{d\varphi(x,t)}{dt} = -\frac{1}{2}\frac{\partial^2\varphi(x,t)}{\partial^2 x} + u(x)\varphi(x,t),\ \ (x,t) \in [0, 2\pi L) \times [0, T], \tag{D.5}$$

where the initial periodic function $\varphi_0(x)$ is the approximate periodic function of $\psi_0(x)$. We use the periodic Fourier pseudospectral method and the OS2 method to discretize (D.5) in space and time directions, respectively. Since the PAM can use one-dimensional FFT to solve (D.5) and the number of grid points is $2ML$, then the computational complexity is $O((2ML)\log(2ML))$ of each time step.

REFERENCES

[1] H. Poincaré, *Sur le probléme des trois corps et les équations de la dynamique*, Acta Math., 13 (1890), pp. A3–A270.

[2] D. Shechtman, I. Blech, D. Gratias, and J. Cahn, *Metallic phase with long-range orientational order and no translational symmetry*, Phys. Rev. Lett., 53 (1984), pp. 1951–1953.

[3] Y. Cao, V. Fatemi, S. Fang, K. Watanabe, T. Taniguchi, E. Kaxiras, and P. Jarillo-Herrero, *Unconventional superconductivity in magic-angle graphene superlattices*, Nature, 556 (2018), pp. 43–50.

[4] A. Sutton, *Irrational interfaces*, Prog. Mater. Sci., 36 (1992), pp. 167–202.

[5] M. Baake and U. Grimm, *Aperiodic Order*: *Volume* 1, *A Mathematical Invitation*, Cambridge University Press, 2013.

[6] T. C. Lubensky, *Symmetry, elasticity, and hydrodynamics in quasiperiodic structures*, in Aperiodicity and Order: Introduction to Quasicrystals 1, M. V. Jaric, ed., 1988, pp. 199–280.

[7] H. Bohr, *Almost Periodic Functions*, Chelsea, New York, 1947.

[8] A. Besicovitch, *Almost Periodic Functions*, Dover Publications, New York, 1954.

[9] B. Levitan and V. Zhikov, *Almost Periodic Functions and Differential Equations*, Cambridge University Press, 1982.

[10] K. Jiang and P. Zhang, *Numerical mathematics of quasicrystals*, Proc. Int. Cong. Math., 3 (2018), pp. 3575–3594.

[11] K. Jiang, S. Li, and P. Zhang, *On the Approximation of Quasiperiodic Functions with Diophantine Frequencies by Periodic Functions*, preprint, arXiv:2304.04334, 2023.

[12] K. Jiang and P. Zhang, *Numerical methods for quasicrystals*, J. Comput. Phys., 256 (2014), pp. 428–440.

[13] K. Barkan, M. Engel, and R. Lifshitz, *Controlled self-assembly of periodic and aperiodic cluster crystals*, Phys. Rev. Lett., 113 (2014), 098304.

[14] K. Jiang, J. Tong, P. Zhang, and A. Shi, *Stability of two-dimensional soft quasicrystals in systems with two length scales*, Phys. Rev. E, 92 (2015), 042159.

[15] Y. Zhou, H. Chen, and A. Zhou, *Plane wave methods for quantum eigenvalue problems of incommensurate systems*, J. Comput. Phys., 384 (2019), pp. 99–113.

[16] X. Li and K. Jiang, *Numerical simulation for quasiperiodic quantum dynamical systems*, J. Numer. Methods Comput. Appl., 42 (2021), pp. 3–17 (in Chinese).

[17] Z. Gao, Z. Xu, Z. Yang, and F. Ye, *Pythagoras superposition principle for localized eigenstates of two-dimensional moiré lattices*, Phys. Rev. A, 108 (2023), 013513.

[18] C. Wang, F. Liu, and H. Huang, *Effective model for fractional topological corner modes in quasicrystals*, Phys. Rev. Lett., 129 (2022), 056403.

[19] D. Cao, J. Shen, and J. Xu, *Computing interface with quasiperiodicity*, J. Comput. Phys., 424 (2021), 109863.

[20] K. Jiang, W. Si, and J. Xu, *Tilt grain boundaries of hexagonal structures: A spectral viewpoint*, SIAM J. Appl. Math., 82 (2022), pp. 1267–1286.

[21] C. Canuto, M. Hussaini, A. Quarteroni, and T. Zang, *Spectral Methods: Fundamentals in Single Domains*, Springer, Berlin, 2006.

[22] P. Bohl, *Über die Darstellung von Funktionen einer Variablen durch trigonometrishe Reihen mit mehrer Variablen proportionalen Argumenten*, Dorpat/Tartu, 1893.

[23] H. Bohr, *Zur Theorie fastperiodischer Funktionen* I-II, Acta Math., 45 (1925), pp. 29–127 and 46 (1925), pp. 101–214.

[24] R. Iannacci, A. Bersani, G. DeIl'Acqua, and P. Santucci, *Embedding theorems for Sobolev-Besicovitch spaces of almost periodic functions*, Z. Anal. Anwend., 17 (1998), pp. 443–457.

[25] C. Corduneanu, *Almost Periodic Functions*, 2nd ed., Chelsea, New York, 1989.

[26] P. Walters, *An Introduction to Ergodic Theory*, Springer, Berlin, 1982.

[27] H. Pitt, *Some generalizations of the ergodic theorem*, Math. Proc. Cambridge, 38 (1942), pp. 325–343.

[28] Y. Meyer, *Algebraic Numbers and Harmonic Analysis*, North-Holland, Amsterdam, 1972.

[29] B. Yann, *Approximation by Algebraic Numbers*, Cambridge University Press, 2004.

[30] P. Wang, Y. Zheng, X. Chen, C. Huang, Y. Kartashov, L. Torner, V. Konotop, and F. Ye, *Localization and delocalization of light in photonic moiré lattices*, Nature, 577 (2020), pp. 42–46.

[31] J. Bourgain and W. Wang, *Anderson localization for time quasi-periodic random Schrödinger and wave equations*, Comm. Math. Phys., 248 (2004), pp. 429–466.

[32] T. Wang, H. Chen, A. Zhou, and Y. Zhou, *Layer-Splitting methods for time-dependent Schrödinger equations of incommensurate systems*, Commun. Comput. Phys., 30 (2021), pp. 1474–1498.

[33] M. Frigo and S. Johnson, *The design and implementation of FFTW*3, Proc. IEEE, 93 (2005), pp. 216–231.